THE INSTITUTE OF PAPER CHEMISTRY

Appleton, Wisconsin

THE INTERACTION OF MICROWAVE RADIATION WITH PAPER-WATER SYSTEMS

Project 3322

Report One

A Progress Report

to

MEMBERS OF THE INSTITUTE OF PAPER CHEMISTRY

October 13, 1978

TABLE OF CONTENTS

THE INSTITUTE OF PAPER CHEMISTRY

Appleton, Wisconsin

THE INTERACTION OF MICROWAVE RADIATION WITH PAPER-WATER SYSTEMS

SUMMARY

The interaction of paper-water systems with microwave radiation is exploited in two different paper industry applications: microwave moisture gages and microwave driers. The successful operation of such devices depends upon the large real and imaginary parts of the dielectric constant of water at microwave frequencies. The driers function because the imaginary part results in heat generation, while different moisture gages rely on differing combinations of both parts.

The goal of this project was to measure the dielectric constant of paper as affected by environment, additives, and papermaking processes. This is intended to better define the basic interaction between paper and microwave radiation, so that moisture gages and driers can be more effectively designed, evaluated, and used.

An apparatus for measuring the dielectric constant of thin materials in the X-band frequency range has been designed and constructed. It utilizes a slotted line which, although tedious to operate, provides unequaled accuracy. To further increase sensitivity and accuracy, a computer simulation of a graphical method for statistically analyzing slotted line data has been developed. The result is a system that measures the dielectric constant of thin sheets to an estimated uncertainty of $\pm$ 0.05.

A number of interesting properties of paper have been discovered:

1. The real part of the dielectric constant is about 2.0 for oven dry kraft pulps (at 9.6 GHz), and is slightly less for high yield pulps. The imaginary part of the dielectric constant for all oven dried pulps is very small, i.e., they may be considered lossless.

2. In the frequency range studied, the changes in dielectric constant as a function of frequency are in the same direction as for liquid water.
3. The real and imaginary parts of the dielectric constant plotted against moisture content display a concave shape. This can be interpreted in terms of an increase in the proportion of free water in the system, or to the geometry of the fiber-water-air mixture.
4. Increasing temperature causes an increase in dielectric constant, especially at high moisture contents.
5. Basis weight effects on the dielectric constants (at least for newsprint samples) are small.
6. Wet pressing and refining both cause increases in the measured dielectric constants, but the increases can be explained in terms of the increased density resulting from these operations.
7. Increases in dielectric constant resulting from calendering cannot be explained in terms of an increase in density.
8. The effect of TiO_2 on the measured dielectric constant is very small. This result is surprising since TiO_2 has a dielectric constant greater than water at these microwave frequencies.
9. In machine made papers the dielectric constants are greater in the machine direction than in the cross machine direction. This anisotropy is believed to arise from the in-plane fiber orientation. Since drying restraints are not involved, the ratio of machine to cross-machine direction dielectric constant may provide a measure of fiber orientation.

INTRODUCTION

The moisture content of paper webs and felts can be found indirectly by a variety of methods, but no single method can be utilized with reasonable accuracy for all paper grades over a broad moisture range, e.g., one percent to near saturation. Microwave techniques have the potential, however, of allowing measurements over a very broad range of basis weight and moisture content. In addition, microwave driers have the very desirable feature of selectively drying wet streaks.

The microwave region of the electromagnetic spectrum lies between the radio wave region and the infrared, extending in frequency from about 10^9 to 10^{11} Hertz. Like all electromagnetic radiation, microwaves may be reflected, refracted, diffracted, or scattered. Microwaves penetrate most nonmetallic materials, a feature which permits various applications in nondestructive testing.

Water displays an interesting behavior in the microwave region in that it has a very high dielectric constant and loss factor compared to most materials in which it is found. The water molecule is a good absorber of microwaves, and this allows the continuous and instantaneous determination of moisture content for many materials. The high loss factor of water is primarily attributed to the induced rotation of the water molecule. The free water molecule possesses a large permanent dipole moment, which responds easily to the changing electric field vector at frequencies below the microwave region of the electromagnetic spectrum. At microwave frequencies, however, these polar groups cannot respond as easily to the field, and an absorption of energy results, peaking at slightly above 10^{11} Hertz. Any interference with dipole reorientation will alter the absorption with respect to that of free water.

Cellulose is a material which can influence the absorption. In materials containing polar groups, such as hydroxyl groups in cellulose, it is possible that some of the water present will be bound to these groups via hydrogen bonding. Such bonding could restrict the rotational absorption of energy of the water molecule. Accordingly, this fraction of bound water must be taken into account.

Another method of determining moisture levels by microwave measurements exploits the previously mentioned fact that the dielectric constant of water is still high at low microwave frequencies. The insertion of a lossy dielectric material into a microwave cavity will result in energy losses (as described above) but will also result in a shift of the resonant frequency of the cavity. The perturbation of the resonant frequency of a microwave cavity is dependent on both the volume and dielectric constant of the perturbing material. Since these are affected by the amount of water present, the frequency shift resulting from the introduction of the sample is a measure of the moisture content. As before, however, other web variables can strongly influence the measured moistures.

Surprisingly, very little is known about the microwave-paper interaction. Relatively few studies have been published dealing with the fundamental parameters critical to the optimization of microwave moisture gage performance, or with respect to microwave (and radio-frequency) paper machine driers.

OBJECTIVE

The objective of this program is to measure changes in permittivity, at microwave frequencies, attributable to certain process variables. The fundamental parameters associated with the paper-water systems which are of interest are the real and imaginary parts of a complex permittivity. These are related to the dielectric constant and loss tangent. In addition to the water constant of the sheet, they are dependent upon the manner in which the water is held by the sheet and on the structure and composition of the paper. Other normal sheet components, such as fillers, might also be expected to influence the measured permittivities. At present there seems to be no complete theory which relates the permittivities of the components to those of the composite. One aspect of the work described here was to obtain sufficient data, with reasonable accuracy, so that inferences could be made concerning the effects of the components on the response of the composite.

BACKGROUND

When discussing the interaction of microwave radiation with matter it is necessary to talk in terms of a complex permittivity (or complex dielectric constant). The meanings and significance of these terms, especially when applied to a heterogeneous material such as paper, are presented here.

Complex permittivity is perhaps most easily understood by considering a parallel plate capacitor. If a capacitor with a vacuum dielectric (void) is connected to a sinusoidal voltage source,

$$V = V_o \exp(i\omega t)$$

it will store a charge,

$$Q = C_o V.$$

C_o is called the geometrical (or vacuum) capacitance of the capacitor, and, fringing effects neglected, is equivalent to $\varepsilon_o A/d$ where ε_o is the permittivity of free space, A the surface area of one capacitor plate, and d the distance between plates. In this case the charging current

$$I_c = \frac{dQ}{dt} = i\omega C_o V$$

$$= I_o \exp[i(\omega t + \frac{\pi}{2})]$$

leads the voltage by a phase angle of 90°.

If the capacitor is filled with some substance, the capacitance increases to

$$C = C_o \varepsilon'$$

where ε' represents the real part of the dielectric constant. In addition to the charging current there now appears a loss current, so that the total current is

$$I_t = I_c + I_l.$$

In other words, the capacitor can be characterized by a loss parameter as well as a capacitance parameter. This loss parameter, in part, arises because dipoles, induced in the material as a result of the impressed voltage, are hindered in their attempt to follow or align themselves within the applied field. The loss may be represented as either a series or parallel resistance.

In the parallel circuit of Fig. 1, R represents the loss component (Joule heating, hysteresis losses, etc.) and C the pure capacitive component. The loss current, I_l, is expressible as

$$I_l = \frac{V}{R},$$

so that the total current traversing the capacitor is

$$I_t = (i\omega C + \frac{1}{R})V.$$

A vector diagram for this parallel circuit is shown in Fig. 2. In the figure θ is the phase angle. Since a finite time is required for the dipoles to align with the applied field, the current no longer leads the voltage by $\pi/2$. It is customary to describe the charging current and the loss current by the introduction of a complex dielectric constant.

$$\varepsilon = \varepsilon' - i\varepsilon'',$$

or a complex permittivity, $\varepsilon\varepsilon_o$.

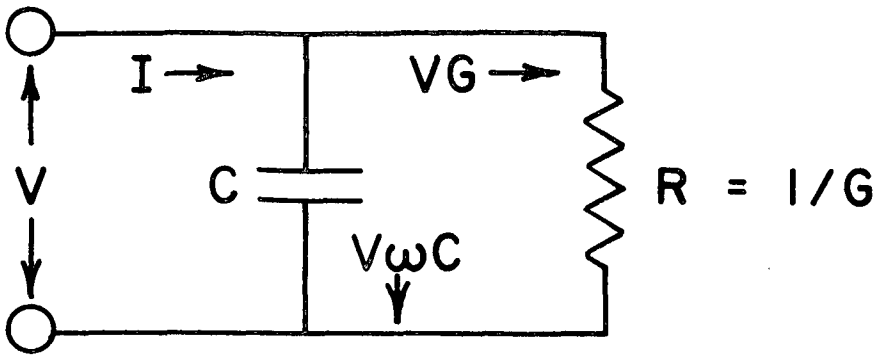

Figure 1. Schematic Circuit Depicting Charging and Loss Currents

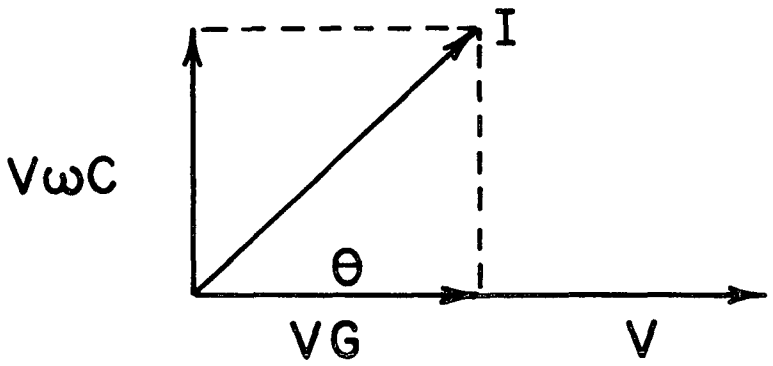

Figure 2. Vector Representation of Figure 1

The total current may now be written

$$I_t = i\omega C_o \varepsilon V.$$

If the frequency is increased to higher and higher values, a point is eventually reached where the time required for electromagnetic disturbances to propagate through a system is no longer small compared to the period of oscillation. When this occurs the low frequency description just given is invalid, and Maxwell's equations must be applied with the appropriate boundary conditions [e.g., see Reference (1)]. At microwave frequencies, disturbances propagate on the order of one centimeter in one period, and Maxwell's equations must be used to characterize systems of centimeter and greater dimensions.

In an infinite free space the sinusoidal solutions to Maxwell's equations are plane waves with wavelength, $\lambda = 2\pi/\omega(\varepsilon_o \mu_o)^{1/2}$, where μ_o is the magnetic permeability of free space. The phase velocity of the plane wave is $\frac{\omega\lambda}{2\pi}$ or $1/(\varepsilon_o \mu_o)^{1/2}$. When electromagnetic waves propagate through dielectrics, $\varepsilon\varepsilon_o$ replaces ε_o in these expressions, resulting in a lower velocity than in free space. Also, the imaginary part of ε makes λ imaginary, and the amplitude of the wave decreases exponentially. As in the low frequency analysis, ε'' results in a loss of energy in the form of heat.

Microwave energy can be propagated in rectangular waveguides. Here sinusoidal solutions to Maxwell's equations are found that meet the boundary conditions imposed by the waveguide. There are many modes of propagation in a waveguide. Each mode has a cutoff frequency below which it decays exponentially along the waveguide and cannot propagate. For simplicity, rectangular waveguides are employed in a frequency range where only one mode (the principal mode) can propagate. In a dielectric filled waveguide the wavelength of the principal mode is $2\pi/(\varepsilon\varepsilon_o \mu\omega - 4\pi^2/\lambda_c^2)^{1/2}$, where λ_c is the cutoff wavelength of the waveguide. As before, a complex permittivity will result in

a shorter wavelength and in energy losses. Complete discussions of dielectric behavior are provided by standard electromagnetic field theory texts (1, 2).

DIELECTRIC CONSTANTS OF COMPOSITE SYSTEMS

When a material is a heterogeneous mixture of substances of differing dielectric constants, an effective dielectric constant of the mixture can be described. The mixture is placed between capacitor plates and the charge required to obtain a certain voltage is measured. The effective dielectric constant, ε_e, of the mixture is said to equal that of a homogeneous material which requires the same charge and voltage. If the detailed geometry of the mixture is known, ε_e can be calculated from the dielectric properties of the constituents by solving the differential equation, $\vec{\nabla}\cdot\varepsilon\nabla\vec{V} = 0$, subject to the boundary conditions at the plates. The dielectric constant at a particular point, ε, can vary throughout the mixture. If it is known, a solution for V can be found, and the charge may be calculated from the integral $\int\varepsilon\nabla\vec{V}\cdot d\vec{A}$ over any surface between the plates. The effective dielectric constant, ε_e, is then found from the ratio of charge to plate voltage drop.

It happens that ε_e depends not only on the dielectric constant of each component and its relative abundance, but also on the geometry of the mixture. This important point can be demonstrated by considering two simple mixtures as shown in Fig. 3. Mixture 1 is made from sheets of two substances of different dielectric constants (ε_1 and ε_2) stacked so that the sheet normals are along the electric field. In mixture 2 the sheet normals are perpendicular to the field. The first case is equivalent to a set of capacitors in series and $1/\varepsilon_e = q/\varepsilon_1 + (1-q)/\varepsilon_2$, where q is the volume fraction of ε_1. In the second case the capacitors are in parallel, so $\varepsilon_e = q\varepsilon_1 + (1-q)\varepsilon_2$. The effective dielectric constant for the parallel case is always greater than for the series alignment, even though both mixtures have the same portion of constituents. Physically, the reason the parallel mixture is more effective is that

the high dielectric portion provides continuous paths of low impedance along the field lines. In the series case the field lines are always broken by low dielectric constant regions resulting in concentration of the field in regions of high impedance. It can be proved (3) that the parallel and series alignments are the extreme situations, and that any other mixture of the same portions must have a value of ε_e intermediate to these extremes.

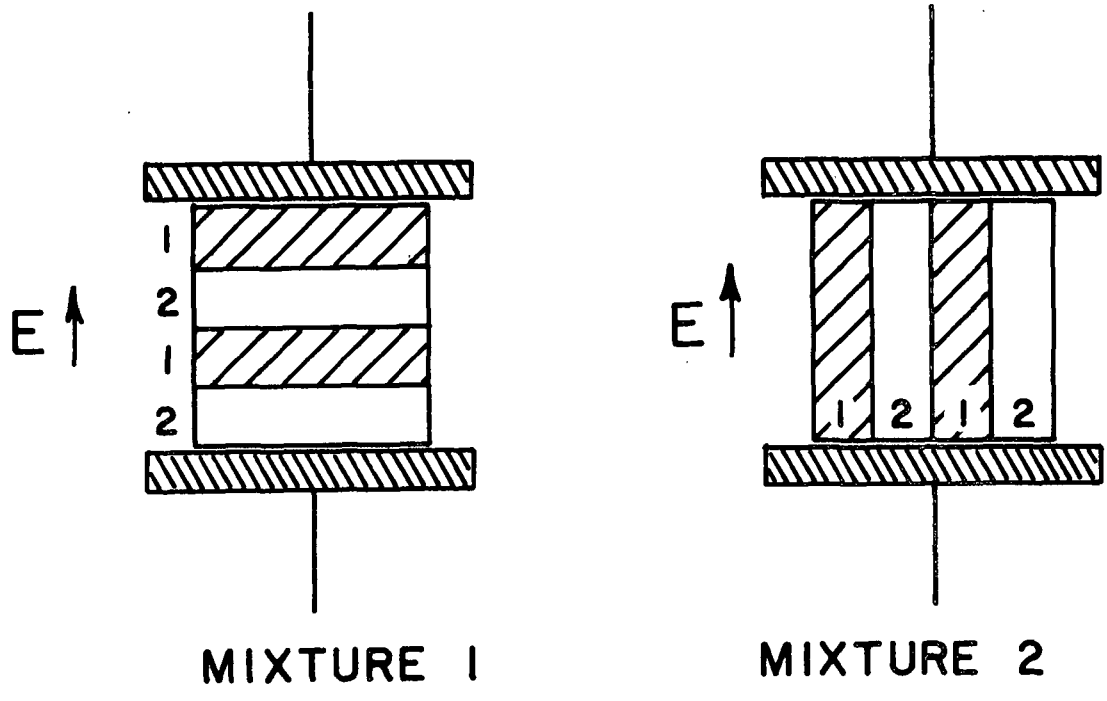

Figure 3. Two Simple Mixtures (see text)

Paper is, of course, a heterogeneous mixture of substances having different dielectric constants. Basically it can be thought of as a mixture of fiber, air, and water. The dielectric constant of water is much greater than the dielectric constants of the other two components. Therefore, the value of the effective dielectric constant for paper depends largely on the amount of moisture and how it is distributed through the sheet. In addition, the polarizability of the H_2O molecule is different when it is absorbed by the fiber, compared to the liquid state, and this

must be considered. The dielectric properties of proteins are explained (4) by dividing the water present into two parts: a shell of "bound" water surrounding the protein molecule and a region of "free" water having the dielectric properties of liquid H_2O. The major dielectric difference between bound and free water is the frequency at which rotation of the permanent dipole moment relaxes. As discussed earlier, at low frequencies, water molecules (bound or free) have permanent dipole moments which can rotate with a sinusoidal electric field and contribute to the real part of the dielectric constant, ε'. As the frequency is increased the dipoles begin to trail the field. When this occurs the dipole motion is out of phase with the electric field, resulting in a large imaginary component of the dielectric constant, ε''. The value of ε'' increases with frequency until the dipoles can no longer keep up with the rapidly changing field, and the contribution of the dipoles to ε' decreases. The imaginary part of the dielectric constant has a resonance peak in the relaxation region as ε' is decreasing. Free water dipoles relax at about 20 GHz, while the bound water in proteins relaxes nearer 1 GHz. Assuming the water bound to cellulose behaves in a similar manner, different contributions from bound and free water are expected in microwave permittivity experiments.

EXPERIMENTAL

EXPERIMENTAL METHOD

The experimental objective of the project is to design and construct an instrument which can measure the permittivity of thin plates with maximum accuracy. The interaction of the sample and the microwave radiation must be mathematically defined so that a permittivity can be determined from the measurements. This is not the case with moisture gages, whose output can be calibrated from the readings of samples with known moisture content. Even though a microwave moisture gage responds to changing permittivity, its design will be quite different from a laboratory instrument used to measure permittivity.

After considering a number of alternatives, a "slotted line" technique was chosen for our measurements. A slotted line is a section of rectangular waveguide with a slot in the middle of one side, parallel to the propagation direction. Since the principal mode current is parallel to the slots, it causes no first order perturbation in the electromagnetic field and its effect can be ignored. A small probe, that responds to the electric field strength, is inserted in the slot. The probe is mounted on a carriage that allows it to traverse the slot at a constant insertion depth. The form of the electric field in the waveguide can be determined from the probe current, as the probe moves along the slot. When combined with precision micrometers, slotted line techniques provide very accurate measurements of small field changes. A single apparatus can be used over a moderate frequency range and the cost of such a system is modest. The major drawback to slotted line techniques is that data taking is tedious and time consuming. In the case of a laboratory instrument, one can live with this inconvenience.

In the particular slotted line method used in this work, a moveable short with micrometer control is used to terminate the waveguide. A short is merely a conductor with a flat edge at right angles to the waveguide walls. It is machined to closely fit in the waveguide. The short imposes a boundary condition of zero electric field along its surface. When a plane wave is incident on the short, it is completely reflected. The incident and reflected waves form a standing wave pattern. The resulting electric field is null at the short and at every half wavelength increment in front of the short.

A schematic diagram of the experimental apparatus used in this work is shown in Fig. 4. The frequency range employed is the X-band, extending from about 8.2 to 12.4 GHz. The permittivity of a paper specimen is determined from its effect on the standing wave pattern in the shorted waveguide. The sample is placed in the waveguide with its face normal to the microwave radiation, between the moveable short and the slotted waveguide. The moveable short is attached to a precision micrometer, as is the detector probe in the slotted line. Energy is supplied to the waveguide by a Polarad* 1108A variable frequency microwave signal generator, with internal 1000 Hz square wave amplitude modulation, after passing through a Hewlett Packard** 11686 A low pass filter. The signal is picked up by the probe, rectified by an Alpha Industries*** DDC4561D Low Barrier Schottky Diode (LBSD) in the probe mount, and sent to a Hewlett Packard** 415E Standing Wave Ratio (SWR) meter which has a 1000 Hz bandpass filter. The combination of 1000 Hz signal modulation and 1000 Hz receiver filter is used to improve the noise to signal ratio. All waveguide and other components were commercially available, but it was necessary to modify the probe carrier

*Polarad Electronic Instruments, 5 Delaware Dr., Lake Success, NY 11040.
**Hewlett Packard, 1820 Embarcadero Rd., Palo Alto, CA 94303.
***Alpha Industries, Inc., Woburn, MA 01801.

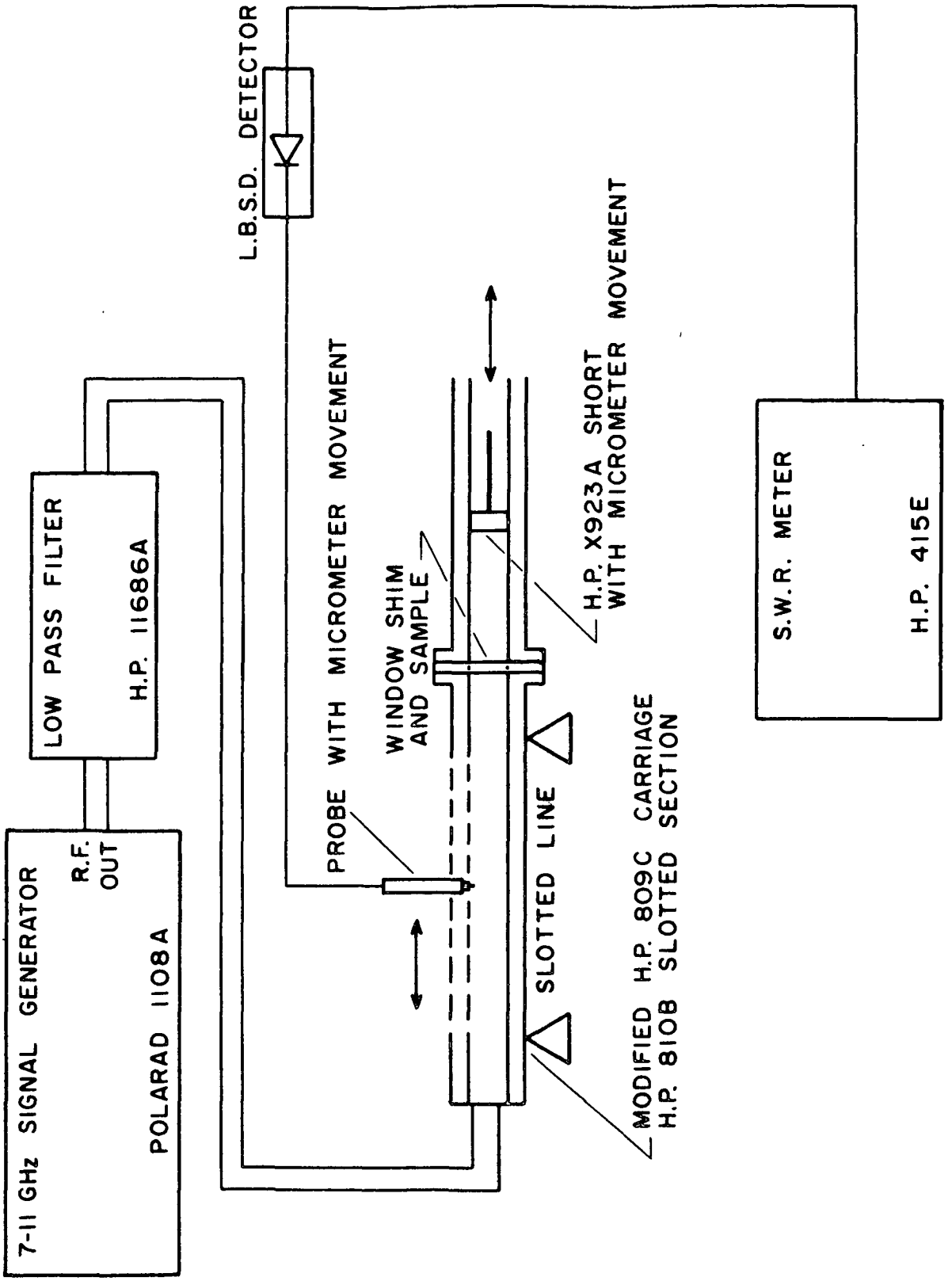

Figure 4. Schematic of Experimental Apparatus

and moveable short in order to use micrometers with 0.0001 inch dial divisions. These micrometers were necessary to provide the accuracy needed when working with thin sheets.

If the shorted waveguide is empty (no sample in place), a near perfect standing wave results from the interference between the incoming wave and the wave reflected by the short. The reflection coefficient, Γ, is defined as the ratio of the reflected to the incident wave. The absolute value of Γ is one at all points along the empty waveguide, but its phase angle varies from π at the nodes to zero at the antinodes. If N measurements of Γ were made at some point as the short was moved through distances, $d = i\lambda/2N$, where $i = 0,\ldots N-1$, the values of Γ, w[illegible] in the complex plane, would lie on the unit circle $2\pi/N$ radians apart. Thi[illegible] is shown in Fig. 5, with $N = 8$.

If a sheet of paper is now inserted in the waveguide, between the [illegible] and the short, radiation reflected and absorbed by the sheet will rotate the Γ's [illegible] move them inside the unit circle. The decrease in wavelength in the sheet causes t[illegible] rotation, while the decrease in the absolute value of Γ is due to losses in the sheet. The magnitude of the effect on the value of Γ also depends on the spatial relationship between the paper and the resulting standing wave pattern. For example, the paper will have a larger effect on Γ if it is placed near an antinode of the empty waveguide. Although the value of Γ is a complicated function of paper thickness and the real and imaginary parts of the permittivity, it is conceptually helpful to picture the real part of ϵ as rotating Γ and the imaginary part as decreasing $|\Gamma|$.

The total effect of a substance in a waveguide may be characterized at some plane by a scattering matrix, S_{ij}, where $i,j = 1,2$. The scattering matrix relates the incident and reflected parts of the total input and output voltages. This is illustrated in the representation of a scattering network shown in Fig. 6. With reference to this

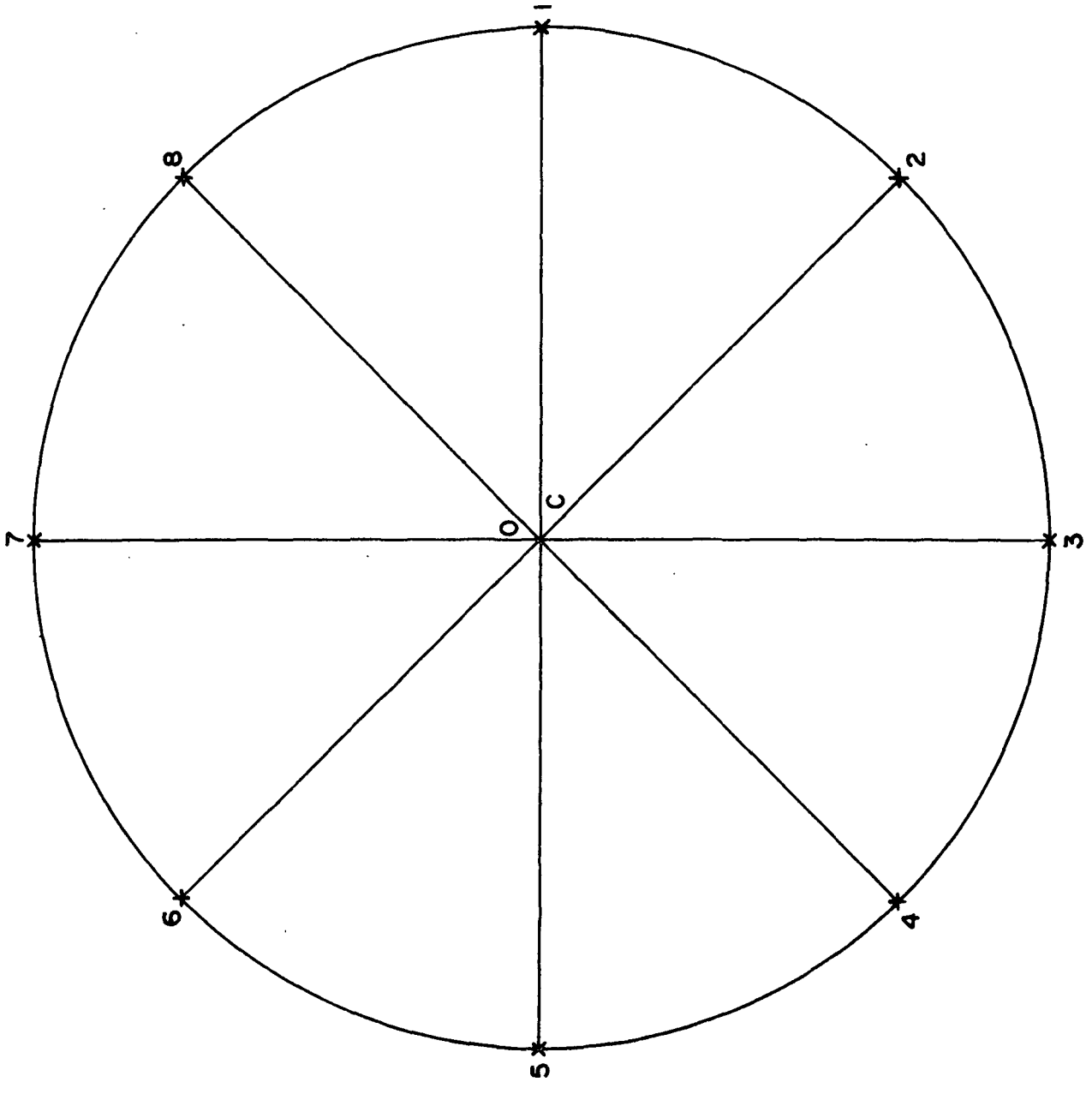

Figure 5. Reflection Coefficient Construction for Empty Waveguide

figure, a_1 and a_2 are the incident voltage amplitudes for the indicated directions, and b_1 and b_2 are the reflected voltage amplitudes in the directions indicated. These latter four quantities are related through the scattering matrix:

$$b_1 = S_{11}a_1 + S_{12}a_2$$

$$b_2 = S_{21}a_1 + S_{22}a_2.$$

Thus the scattering matrix, S_{ij}, is the ratio (at the plane) between radiation entering the substance on the j-side and exiting from the i-side, when the waveguide is terminated in its characteristic impedance on the side opposite j. The interested reader will find a complete description in Reference (5).

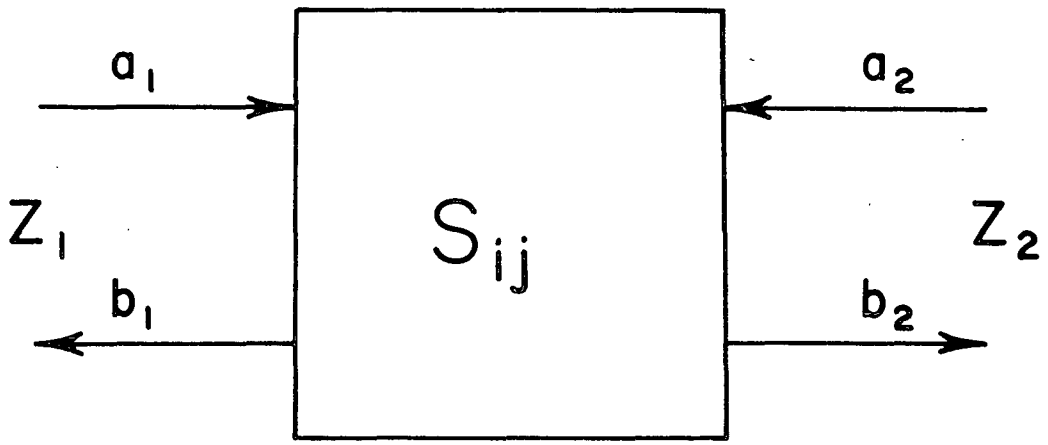

Figure 6. Scattering Network Representation

A graphical technique (5, 6) has been developed to determine the scattering matrix, at a plane a known distance from the first position of the short, using the values of Γ at the previously described N locations of the short. If the Γ's are plotted on the complex plane they are found to lie on a circle with a radius no longer one and whose center, C, is moved away from the unit circle origin. This is depicted in Fig. 7, again with N = 8. When lines between opposite data points are constructed, they are found to intersect at a single point, 0. The graphical technique for finding

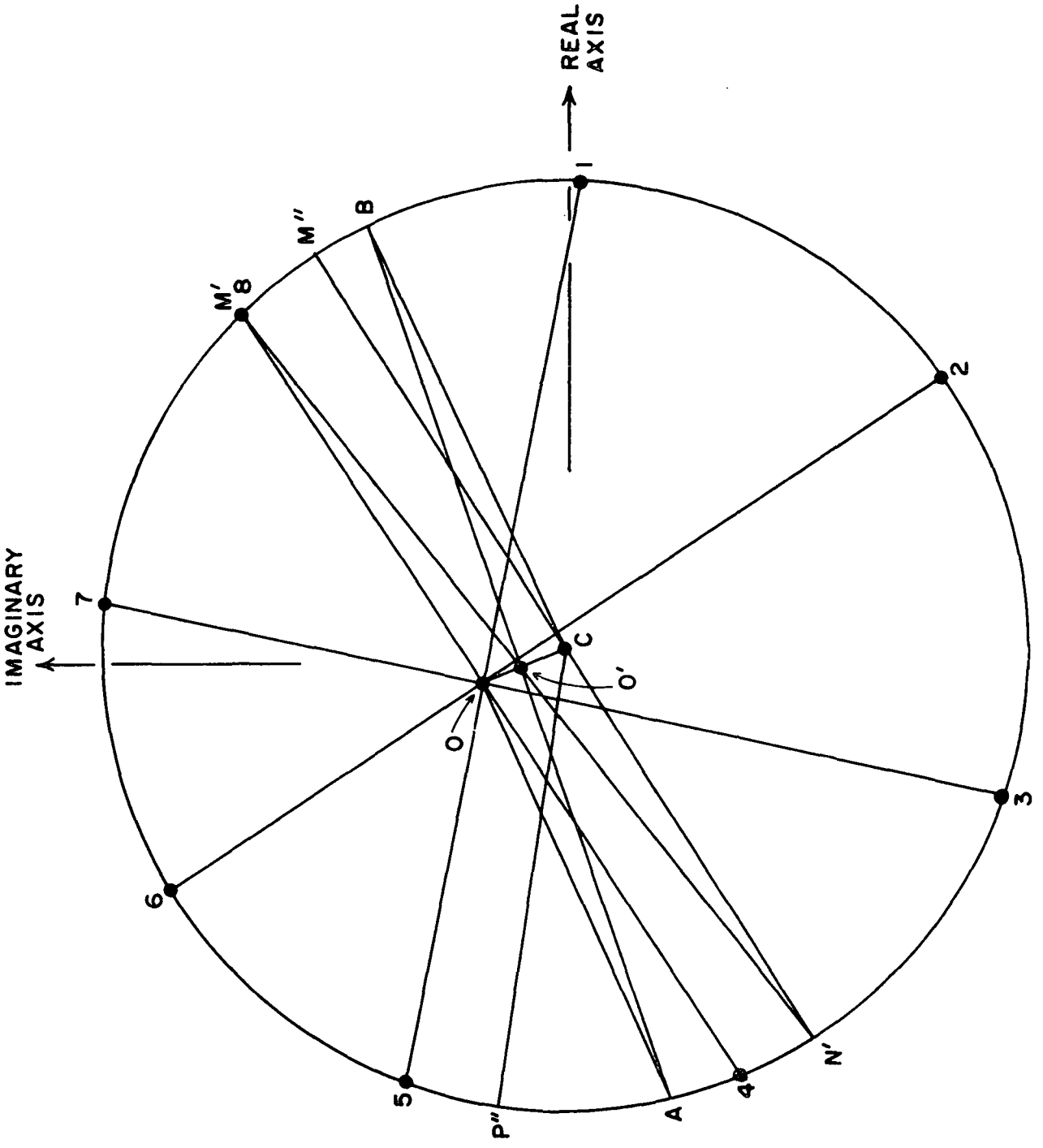

Figure 7. Reflection Coefficient Construction for Waveguide with Paper

S_{ij} relative to the first position of the short then proceeds as follows. Referring to Fig. 7:

(1) a line is drawn between C and O;

(2) perpendiculars are drawn to this line in opposite directions at points C and O (lines $\overline{OA}$ and $\overline{CB}$);

(3) another line is drawn between the points of intersection of the two perpendiculars and the circle (points A and B);

(4) the point, O', is determined by the intersection of the lines $\overline{CO}$ and $\overline{AB}$, constructed in steps 1 and 3;

(5) the absolute value of S_{11} is calculated by measuring the length of $\overline{O'O}$, while the absolute value of S_{22} is equal to the length of $\overline{O'C}$ divided by the radius of the circle;

(6) the phase of S_{11} is found by taking the phase of O' and adding π;

(7) the absolute value of S_{12} is found by measuring the distance from O' to the circle along a perpendicular to the line in step 1 and dividing by the square root of the radius of the circle;

(8) a line is now drawn from the data point closest to the circle, say M' at location 8, through O' to N';

(9) a line is next drawn between C and N' extending to M";

(10) a line is drawn from C at an angle $\frac{\pi(MN-1)}{N}$ from line $\overline{CM"}$, where MN is the data number for M'. In Fig. 7, MN is 8 and the line constructed is $\overline{CP"}$. The angle in question is M"CP", which on Fig. 7 is $7\pi/8$ (since MN = N' = 8);

(11) twice the phase of S_{12} is found by measuring angle OCP";

(12) finally, the phase of S_{22} is found by measuring the angle between the positive real axis and CP".

For a homogeneous material of known dimension, it is possible to calculate the permittivity from the scattering matrix. In fact, there is enough information so that the permittivity can be found either without knowing sheet thickness or without knowing the distance of the sheet from the S_{ij} reference plane. For example, if the reference plane is measured from the right side of the sheet, the thickness can be found by transforming S_{11} such that it equals S_{22}. The absolute value of S_{11}, by symmetry, equals that of S_{22} for a homogeneous sheet, but the phase depends on the relation of the reference frame to each edge. The thickness of sheet, therefore, can be calculated from the phase difference between S_{11} and S_{22}.

If paper were homogeneous with well defined boundaries, this technique could be rigorously used to determine a value for the complex permittivity. Unfortunately, paper is a very inhomogeneous material with a poorly defined thickness. Nonetheless, if the paper's measured scattering matrix can be reproduced by a homogeneous sheet of constant thickness, a permittivity number can be associated with the paper. This is possible if $|S_{11}| = |S_{22}|$. In this case the permittivity of the paper would be said to equal that of the fictitious homogeneous sheet. The latter, however, must be constrained by either a value for the thickness or a value for the distance from the sheet to the first location of the short. If it is not, an infinite combination of sheet thicknesses and permittivities can be found which will generate the measured S_{ij}'s. Therefore, in order to associate a unique permittivity value with paper, either its thickness or the location of one of its boundaries must be defined. Since paper caliper and boundary location are equally nebulous concepts, the value of the permittivity determined by this approach will be no better than the number ascribed to either of these.

The calculations necessary to produce the scattering matrix and the complex permittivity from the N-waveguide measurements have been programmed for those cases of known thickness and boundary location. The method gives reasonable results in that: (1) $|S_{11}| = |S_{22}|$, to within 1%; (2) when a boundary is defined by placing the paper next to the original position of the short, the calculated thickness is about 10% larger than the thickness measured by standard caliper gages; (3) the complex permittivities are within the expected range; and (4) the calculated location of the sheet boundary is close to that predicted when the sheet is placed at an arbitrary position and the thickness as measured with a caliper gage is used to constrain the calculations.

For purposes of data collection, the constrained thickness technique was used. The thickness is determined using a standard caliper gage, and this value is used together with the measured scattering coefficient data to compute the permittivity. The advantages of this method (as compared to the constrained boundary method) are (1) the sheet boundary area is not deformed, and (2) the initial short position can be chosen so that the sample is never too close to a waveguide null where the effect of the paper is difficult to measure.

EXPERIMENTAL PROCEDURES

An important aspect of the slotted line technique concerns how the thin specimen is mounted inside the waveguide. In order to get accurate and repeatable results, it is necessary to carefully align the paper in the waveguide without inserting extraneous material that alters the standing wave pattern. This was achieved in the present work by using "window shims" of assorted thicknesses. A window shim has a punched hole with a height equalling that of the waveguide and with a length slightly longer than the waveguide width. The waveguide has dimensions 0.4 by 0.9 inch. The paper specimen is cut to fit tightly in a window shim. The shim thickness is chosen to be slightly smaller than the specimen thickness. The

shim is then clamped between the slotted line and the moveable short (see Fig. 4) providing a firm grip on the paper. There is no first order effect on the standing wave pattern due to the shim, because the currents in the waveguide along the short dimension are parallel to the wall gaps caused by the shim.

For thin sheets (<0.012 inch) the effect of the paper on the standing wave pattern is not large enough to allow accurate measurements of the dielectric constant. Dielectric constant measurements were made on stacks of different thicknesses. It was found that the variation of the dielectric constant was within the expected experimental error, if the sheets were carefully cut and stacked in the window shim. Therefore, measurements on stacks of sheets were used to calculate the dielectric constants of thin sheets.

When making measurements on paper using the slotted line technique, a power level must be chosen that is large enough to give good signal to noise ratio, but small enough so that the sheet is not dried. A similar trade-off is encountered when probe depth is specified. If the probe is too deep in the waveguide, the standing wave pattern is perturbed, and if it is too shallow the signal may be insufficient for accurate measurements. For these reasons a great deal of experimentation is necessary before optimum combinations of power level and probe depth are chosen.

The actual experimentation with a given specimen is carried out in the following manner.

(1) The equipment is assembled with an empty shim (of the appropriate thickness to be used with a given paper specimen) inserted between the slotted line and the variable short.

(2) The wavelength in the slotted line, λ_{SL}, is measured. This is done by measuring the distance traveled by the probe between minimums. The location of minimums is found by (a) visually locating a minimum (with the SWR meter), (b) moving approximately 0.002 inch to one side and recording the reading, (c) moving to the other side of the minimum until an identical reading is found, and (d) averaging the two positions.

(3) The wavelength in the waveguide containing the moving short, λ_{MS}, is measured. This is done by finding the distance the short must move to cause minimums to repeat at a single probe setting.

(4) Construct a SWR calibration curve. This is done by locating a minimum, and then determining the SWR meter readings as a function of distance, d, from the minimum. The values on the two sides of the minimum are averaged. These readings are plotted against $20 \log_{10} \sin (2\pi d/\lambda_{SL}) + C$, where C is chosen so that the X and Y coordinates are equal at large distances from the minimum. A curve is drawn through the points. The meter readings are corrected by using the X coordinate value, corresponding to a Y coordinate equal to the actual reading.

(5) Replace the short at the position of the first reading, about $\lambda_{MS}/16$ from the sheet boundary, and locate the probe at a minimum.

(6) The empty shim is removed by disconnecting the short from the slotted line. A paper specimen is inserted into the shim and it is returned to the system which is then reassembled.

(7) The distance, DP, that the probe must be moved to locate the new minimum is found and recorded.

(8) The distance between 3dB points on the minimum of the standing wave pattern, DX, is then recorded.

(9) Steps (7) and (8) are repeated for each of the N settings. The distance the short is moved between data points is $\lambda_{MS}/2N$.

(10) The DX and DP values at each of the N settings, λ_{SL}, and the paper caliper are then inputed to the computer.

The DX(i) and DP(i) values (where i = 1,2,...N), together with λ_{SL}, are used to determine the polar coordinates R(i) and θ(i) of the N data points:

$$R(i) = [\{\lambda_{SL}/\pi DX(i)\}-1]/[\{\lambda_{SL}/\pi DX(i)\} + 1]$$

$$\theta(i) = 4\pi DP(i)/\lambda_{SL}.$$

The computer program finds the best circle through these data points, and determines the center, C, as well as the point O (refer to Fig. 7). The graphical procedure described in the Experimental Methods section, again with reference to Fig. 7, is then performed to determine the complex elements of the scattering matrix, S_{ij}. In the technique in which the specimen thickness, L, is specified (as it is here) the elements of the scattering matrix are used in conjunction with L and λ_{SL} to calculate the permittivity. Two new complex numbers are defined:

$$S'_{12} = |S_{12}|\exp(i(\arg S_{12} - 2\pi L/\lambda_{SL})),$$

$$S'_{11} = \pm\, |S_{11}|\exp(ARG),$$

where $ARG = \dfrac{\arg S_{11} + \arg S_{22}}{2} - 2\pi L/\lambda_{SL}$.

A new complex number Z is now defined as

$$Z = \frac{(1-S'_{11})^2 - (S'_{12})^2}{(1+S'_{11})^2 - (S'_{12})^2}$$

where the sign used in S'_{11} is that which makes the real part of Z, Re(Z), greater than one. The real and imaginary parts of the complex permittivity are then,

$$\varepsilon' = \frac{\mathrm{Re}(Z) + (\lambda_{SL}/2a)^2}{1 + (\lambda_{SL}/2a)^2},$$

and

$$\varepsilon'' = -\mathrm{Im}(Z)/[1 + (\lambda_{SL}/2a)^2],$$

where a is the width of the waveguide and Im(Z) is the imaginary part of Z. A more complete development of the equations is presented in Reference (5). All calculations are performed by the computer program which is included in Appendix I. The program also provides a simple error analysis.

When N, the number of settings of the short, is greater than 4, the coordinates of C and O can be determined by different sets of data and the average can be taken as the best data point. In the experimental work here, N = 8 was used. This gives enough data points for a good average without making experimentation excessively tedious. With N = 8, C can be calculated 56 different ways and O six different ways. The program gives an estimate of statistical scatter by calculating the value of ε' and ε'' resulting from the scatter in C and O. This is done by finding ε' and ε'' for all combinations of C and O adjusted by plus or minus one standard deviation in the real and imaginary directions. The maximum excursions are recorded. The scatter in ε, determined as above, is used as an estimate of the data quality. Altogether, the slotted line technique offers a variety of parameters for evaluating the data.

These are: (1) ϵ scatter; (2) the difference in $|S_{11}|$ and $|S_{22}|$, and (3) the difference between the distance from the sheet to the first short location as measured and as calculated by the computer. Large values of any of these parameters can come from a number of sources, e.g., poor data taking, sample misalignment, sheet drying (when it is near an electric field antinode), differences between a sheet of paper and a homogeneous dielectric slab, and any imperfections in the waveguide. If any one of these three parameters is considered excessive, the experiment is repeated.

The machine-made papers and handsheets used in the investigation are listed in Table I. The sample numbers are constructed so that the first letter or letters denote the paper type and the three following numbers represent the nominal basis weight in g/m^2. Thus, N refers to a newsprint handsheet, NM to a machine made newsprint, BK to a bleached kraft, KL to a kraft linerboard, UK to an unbleached kraft, and C to a coating raw stock. In the N series, the handsheets were prepared at different basis weights using repulped newsprint. For the BK series, the basis weight was held constant at a nominal value of 60 g/m^2, but the handsheets were either calendered or filled with TiO_2 or clay. For this series, the subnumbers -01 and -02 refer to two levels of calendering, -05 and -15 refer to the percent of TiO_2 added as a filler (by weight), and -10 and -25 refer to the percentage of clay added as filler. Also for the BK series, the subnumbers -04, -08, and -12, refer to weight percentage of TiO_2 retained (per ovendry weight). The kraft linerboard series are machine-made papers with basis weights of 26, 42, 69, and 90 $lb/1000\ ft^2$. The unbleached kraft handsheets have the same nominal basis weight (206 g/m^2) but were wet pressed or refined at different pressures or times, respectively. The C series are hand drawdown clay-latex coatings on a commercial coating grade raw stock. The subscripts -1L and -1H refer to single-side coatings at light and heavy coat weights, and -2L and -2H are coatings on both sides of the sheet at the same light or heavy coat weights.

TABLE I

SAMPLE CHARACTERISTICS

Sample No.	Description	Oven-dry Basis Wt., g/m^2	Wet Pressing Pressure, psi	Ash Content, %	Other
NM052	Machine-made newsprint	44.6			
NO45	Repulped newsprint	43.2	50		
NO55	Repulped newsprint	52.8	50		
NO60	Repulped newsprint	58.5	50		
NO65	Repulped newsprint	61.9	50		
BKO60-00	Bleached kraft (BK)	59.2	50	0.22	
BKO60-01	BK, calendered	59.2	50		One calender pass
BKO60-02	BK, calendered	59.2	50		Three calender passes
BKO60-04	BK, 4% TiO_2 furnish	60.1	50	3.71	
BKO60-08	BK, 8% TiO_2 furnish	60.4	50	8.85	
BKO60-12	BK, 12% TiO_2 furnish	60.9	50	14.43	
BKO60-10	BK, 10% clay furnish	59.3	50	1.72	
BKO60-25	BK, 25% clay furnish	59.3	50	3.65	
KL126	Kraft linerboard	130.5			
KL205	Kraft linerboard	195.8			
KL337	Kraft linerboard	326.6			
KL440	Kraft linerboard	394.4			
UK205-1	Unbleached kraft	199.7	10		Refining time, 5 min
UK205-2	Unbleached kraft	199.8	50		Refining time, 5 min
UK205-3	Unbleached kraft	200.2	84		Refining time, 5 min
UK205-4	Unbleached kraft	200.2	400		Refining time, 5 min
UK205-5	Unbleached kraft	201.0	50		Refining time, 25 min
CO60-0	Uncoated, 25% rag	61.7			
CO60-1L	Coated rag stock (1 side)	72.8			Coating weight, 11.1 g/m^2
CO60-1H	Coated rag stock (1 side)	81.6			Coating weight, 19.8 g/m^2
CO60-2L	Coated rag stock (2 sides)	88.0			Coating weight, 26.2 g/m^2
CO60-2H	Coated rag stock (2 sides)	102.8			Coating weight, 41.1 g/m^2

The effect of orientation of the electric field with respect to the machine direction of machine-made papers (NM052 and KL205) was determined by cutting the samples at different angles to the machine direction. Changes in permittivity with measuring frequency, temperature, and moisture content were also studied.

All specimens were cut to the dimensions of the waveguide. A problem encountered in selecting 0.4" x 0.9" samples to fit in the waveguide was that weight and caliper could vary significantly in the sheet from which the sample was cut. In fact in some cases the variance due to sample location masked the effect caused by process variables. In sample groups having roughly the same basis weight (the BK and UK samples), this problem was minimized by choosing waveguide samples of equal weight. When samples were cut for electric field orientation comparisons, both caliper and weight were equalized.

All experiments were carried out in a controlled environment, with specimens conditioned in this environment for a period of at least 12 hours prior to testing. In the studies of the effects of process variables, fillers, orientation, and frequency, the experiments were performed in an environment of 73°F and 50% RH. For the moisture content studies, experiments were performed with a number of samples at relative humidities of 15, 24, 35, 45, 50, 60, 75, 80, and 90% at 73°F and 35, 50, and 75% at 100°F.

RESULTS AND DISCUSSION

The permittivities of the samples were measured as described earlier. Tables II and III give the results of the experimental measurements. The scatter in the data, as specified in the experimental section, indicates that it is possible to approximate a sheet of paper as a homogeneous dielectric slab with an uncertainty of $\pm$ 0.05 in ε. This represents about 3% of the value of a typical ε' and about 15% of ε''. The effect of changing frequency, over the experimental range of the equipment, is shown in Fig. 8. The behavior is as expected from the measured behavior of liquid water at these frequencies. That is, ε' is expected to decrease with frequency, while ε'' increases. In all of the results discussed below, the frequency was held constant at 9.6 GHz.

Figure 9 shows the effect of moisture content on the permittivity of a newsprint sample. The general concave upward form of the curves is typical of all of the samples tested. There are at least two possible explanations for this behavior. One is that at higher moisture levels a larger portion of the water is "free." As discussed earlier, free water is thought by some authors (4) to have a higher dielectric constant than "bound" water at microwave frequencies. If each additional increment of moisture has a higher dielectric constant, a steadily increasing slope is expected. The second explanation comes from dielectric mixture theory. Paper can be thought of as a heterogeneous mixture of fiber, air, and water. If the geometry of the system could be specified, the effective dielectric constant of the sheet could be calculated from dielectric properties and amount of each constituent present. This is not feasible, but it is possible to infer a trend by studying the properties of other mixtures. When the dielectric constant of a two-component mixture is plotted as a function of the concentration of the higher dielectric constant component, the curve nearly always has an increasing slope.

TABLE II

SUMMARY RESULTS

Sample	Orientation	Frequency, GHz	ODBW, gm/m²	73°F 15% RH Caliper, inch	ε'	ε"	Grav. Moist., %	24% RH Caliper, inch	ε'	ε"	Grav. Moist., %	35% RH Caliper, inch	ε'	ε"	Grav. Moist., %	45% RH Caliper, inch	ε'	ε"	Grav. Moist., %
NM052	∥	9.60	44.6																
NM052	∥	9.60	44.6																
NM052	30°	9.60	44.5																
NM052	60°	9.60	44.8																
NM052	⊥	9.60	44.8																
N045	∥	9.60	43.2	0.0045	1.736	0.072	4.85												
N055	∥	9.60	52.8	0.0056	1.720	0.067	4.40												
N060	∥	9.60	58.5	0.0061	1.700	0.066	4.47												
N065	∥	9.60	61.9	0.0065	1.718	0.057	4.91	0.0064	1.758	0.089	6.00	0.0065	1.883	0.131	7.92	0.0065	1.885	0.139	8.54
N065	∥	8.50	61.9																
N065	∥	9.20	61.9																
N065	∥	9.60	61.9																
N065	∥	9.98	61.9																
N065	∥	10.92	61.9																
BK060-00	∥	9.60	59.2	0.0036	2.289	0.136	3.71	0.0035	2.322	0.134	4.88	0.0036	2.473	0.213	6.31	0.0036	2.570	0.286	6.78
BK060-01	∥	9.60	59.2	0.0030	2.513	0.172	3.81												
BK060-02	∥	9.60	59.2	0.0028	2.565	0.137	3.91												
BK060-10	∥	9.60	59.3	0.0036	2.243	0.142	3.70												
BK060-25	∥	9.60	59.3	0.0036	2.231	0.130	3.70												
BK060-00	∥	9.60	60.0																
BK060-04	∥	9.60	60.1																
BK060-08	∥	9.60	60.4																
BK060-12	∥	9.60	60.9																
UK205-1	∥	9.60	199.7	0.0182	1.797	0.067	4.54												
UK205-2	∥	9.60	199.8	0.0161	1.886	0.070	4.45	0.0162	1.904	0.108	5.65	0.0164	2.058	0.163	6.90	0.0164	2.096	0.186	7.48
UK205-3	∥	9.60	200.2	0.0145	2.001	0.094	4.18												
UK205-4	∥	9.60	200.2	0.0122	2.253	0.106	4.36												
UK205-5	∥	9.60	201.0	0.0131	2.139	0.092	4.08												
KL126	∥	9.60	130.5	0.0078	2.267	0.112	4.12												
KL205	∥	9.60	195.8	0.0118	2.279	0.119	4.33	0.0119	2.393	0.153	5.85	0.0115	2.594	0.252	6.76	0.0116	2.590	0.274	7.37
KL205	30°	9.60	195.7																
KL205	60°	9.60	196.3																
KL205	⊥	9.60	195.9	0.0117	2.233	0.096	4.27	0.0119	2.269	0.138	5.84	0.0115	2.494	0.216	6.58	0.0116	2.500	0.237	7.25
KL337	∥	9.60	326.6	0.0211	2.188	0.095	4.13												
KL440	∥	9.60	394.4	0.0253	2.117	0.076	3.98												
C060-0	∥	9.60	61.7																
C060-1L	∥	9.60	72.8																
C060-1H	∥	9.60	81.6																
C060-2L	∥	9.60	88.0																
C060-2H	∥	9.60	102.8																

TABLE II (Continued)

SUMMARY RESULTS

	73°F																			
	50% RH				60% RH				75% RH				80% RH				90% RH			
Sample	Caliper, inch	ε'	ε"	Grav. Moist., %	Caliper, inch	ε'	ε"	Grav. Moist., %	Caliper, inch	ε'	ε"	Grav. Moist., %	Caliper, inch	ε'	ε"	Grav. Moist., %	Caliper, inch	ε'	ε"	Grav. Moist., %
NM052	0.0032	2.385	0.163	7.96																
NM052	0.0040	2.105	0.188	9.03																
NM052	0.0040	2.072	0.180	9.29																
NM052	0.0040	2.010	0.158	9.13																
NM052	0.0040	1.990	0.145	9.13																
NO45	0.0046	1.901	0.140	8.67													0.0047	2.222	0.342	14.18
NO55	0.0057	1.869	0.153	8.55													0.0058	2.239	0.409	13.56
NO60	0.0063	1.858	0.135	8.77													0.0064	2.266	0.408	13.68
NO65	0.0066	1.928	0.162	8.95	0.0066	1.973	0.188	9.76	0.0066	2.094	0.292	11.71	0.0067	2.205	0.367	12.94	0.0067	2.327	0.456	13.95
NO65	0.0066	1.868	0.098	7.50																
NO65	0.0066	1.832	0.114	7.50																
NO65	0.0066	1.830	0.115	7.50																
NO65	0.0066	1.827	0.117	7.50																
NO65	0.0066	1.810	0.126	7.50																
BK060-00	0.0036	2.662	0.308	7.06	0.0036	2.735	0.394	8.15	0.0037	2.921	0.534	9.40	0.0037	3.138	0.661	11.29	0.0038	3.446	1.018	13.02
BK060-01	0.0030	2.913	0.325	6.97													0.0033	3.646	0.968	12.29
BK060-02	0.0028	2.993	0.309	7.06													0.0031	3.642	0.848	12.37
BK060-10	0.0036	2.599	0.323	6.87													0.0037	3.426	0.965	12.36
BK060-25	0.0037	2.486	0.265	6.96													0.0038	3.302	0.896	11.95
BK060-00	0.0035	2.635	0.334	7.34																
BK060-04	0.0035	2.612	0.287	7.14																
BK060-08	0.0034	2.684	0.281	6.65																
BK060-12	0.0034	2.692	0.258	5.97																
UK205-1	0.0188	1.984	0.179	8.05													0.0196	2.461	0.523	13.36
UK205-2	0.0166	2.146	0.226	8.04	0.0167	2.250	0.292	9.08	0.0169	2.339	0.404	10.77	0.0171	2.489	0.460	11.89	0.0173	2.620	0.585	13.27
UK205-3	0.0150	2.240	0.230	7.79													0.0157	2.916	0.703	13.11
UK205-4	0.0126	2.562	0.292	7.95													0.0132	3.448	0.906	13.32
UK205-5	0.0135	2.430	0.261	7.68													0.0143	3.211	0.824	13.14
KL126	0.0079	2.485	0.210	6.53													0.0085	3.266	0.868	12.48
KL205	0.0116	2.608	0.258	7.59	0.0119	2.745	0.449	8.90	0.0120	2.979	0.593	10.43	0.0128	3.128	0.710	12.31	0.0128	3.516	1.003	14.06
KL205	0.0115	2.628	0.265	7.60																
KL205	0.0116	2.574	0.228	7.30																
KL205	0.0116	2.562	0.225	7.53	0.0119	2.662	0.350	8.84	0.0120	2.801	0.482	10.32	0.0127	2.983	0.590	12.30	0.0130	3.257	0.833	14.01
KL337	0.0213	2.428	0.230	6.93													0.0234	3.072	0.771	13.09
KL440	0.0155	2.375	0.134	6.74													0.0281	2.861	0.607	12.26
C060-0	0.0033	2.801	0.268	5.89																
C060-1L	0.0036	2.856	0.263	5.19																
C060-1H	0.0038	2.810	0.220	4.73																
C060-2L	0.0038	3.053	0.271	4.60																
C060-2H	0.0042	3.140	0.223	3.96																

TABLE III

SUMMARY RESULTS

	100°F											
	35% RH				50% RH				75% RH			
Sample	Caliper, inch	ε'	ε"	Grav. Moist., %	Caliper, inch	ε'	ε"	Grav. Moist., %	Caliper, inch	ε'	ε"	Grav. Moist., %
NO65	0.0064	1.909	0.164	6.76	0.0065	1.861	0.129	7.81	0.0067	2.408	0.478	13.50
BK060-00	0.0036	2.519	0.300	5.65	0.0036	2.597	0.261	6.69	0.0037	3.337	0.808	9.75
UK205-2	0.0163	2.066	0.199	5.73	0.0164	2.172	0.244	6.98	0.0171	2.702	0.587	11.89
KL205	0.0118	2.594	0.252	6.30	0.0118	2.608	0.258	7.09	0.0127	2.979	0.593	12.61
KL205	0.0119	2.494	0.216	6.24	0.0120	2.562	0.225	7.03	0.0129	2.801	0.482	12.50

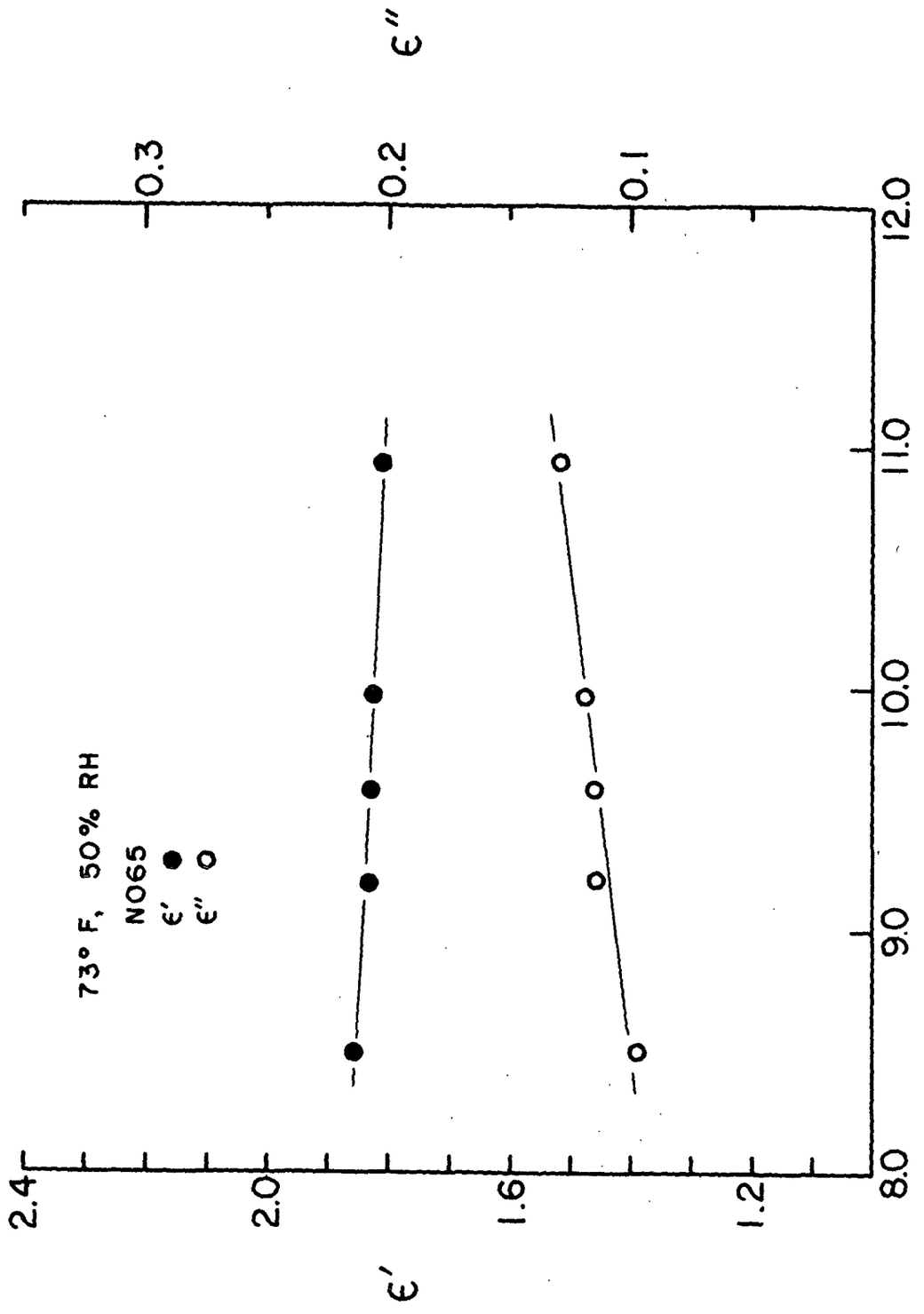

Figure 8. Dielectric Constant vs. Frequency

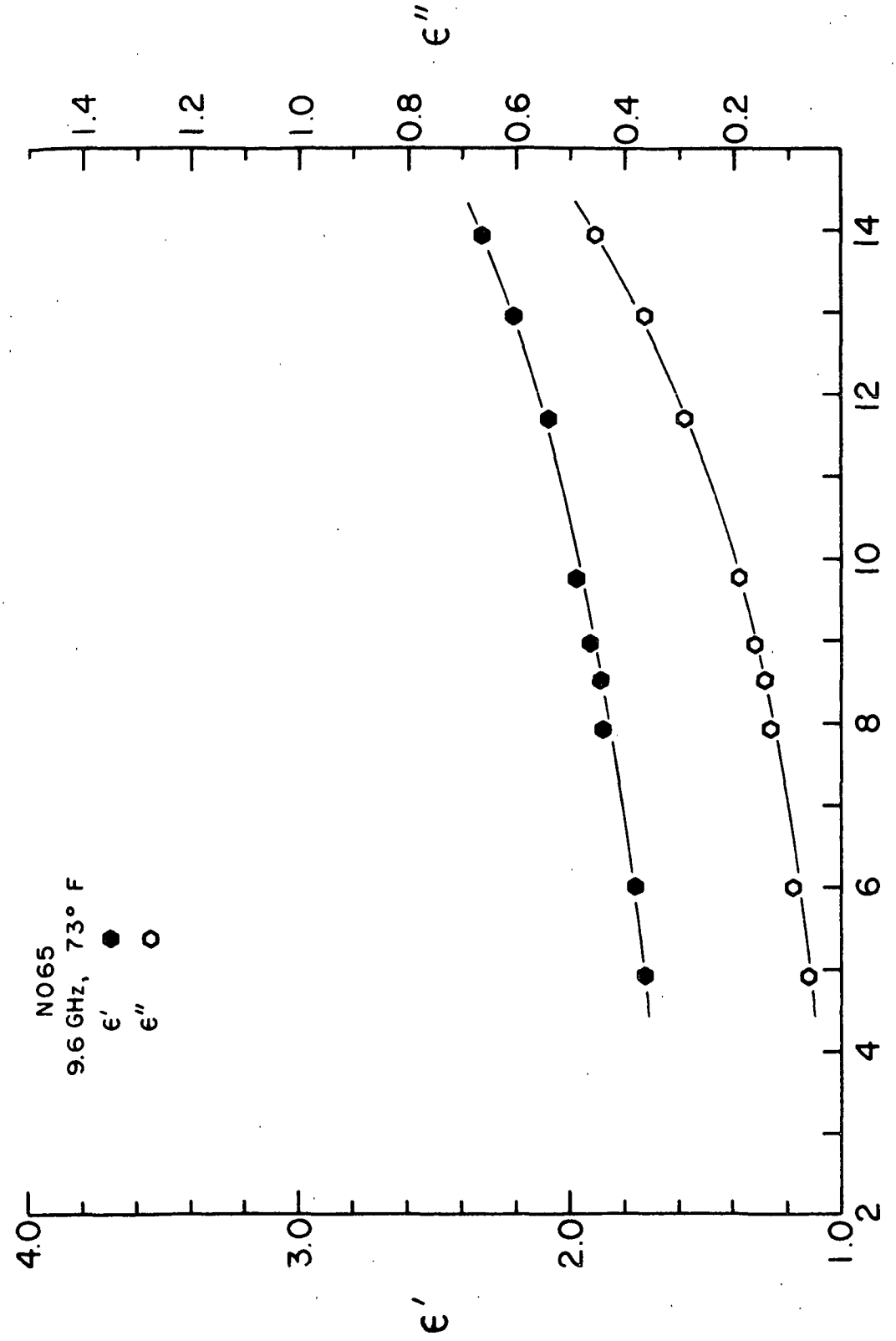

Figure 9. Dielectric Constant vs. Moisture Content

This is because (except in the case of parallel addition) the areas of high permittivity become more contiguous in the electric field direction as concentration increases.

If the curves in Fig. 9 are extrapolated back to zero percent moisture the values for ε' and ε'' are approximately 1.6 and zero, respectively. These "oven dry" values are presumably representative of the cellulose-air fraction of the sheet. (The extent to which "bound water" affects these values, if it is present, is of course uncertain.) The low value of ε'' for the oven dry newsprint implies that cellulose is a very low loss material, at least at the measuring frequency of 9.6 GHz.

Figure 10 is a similar plot for a machine-made kraft linerboard. Linerboard data were not as reproducible as that from the other samples. As a result, they did not fit a smooth curve as closely. This is presumably due to the high degree of two sidedness in these materials. There are two sets of curves presented in Fig. 10, one with the electric field in the waveguide aligned in the machine direction and one in the cross machine direction. These curves demonstrate the anisotropy of the dielectric constant in a machine-made sheet. Notice the dielectric constant is larger in the machine direction. This is caused by the preferred alignment of fibers in this direction. The microwave dielectric properties of a sheet can largely be attributed to the moisture, which in turn acquires a spacial structure from fiber alignment. This anisotropy in the moisture geometry results in dielectric anisotropy. A simplified way of visualizing the effect is to note that the sheet looks more like a distribution of capacitors in parallel to a machine direction electric field, and more like a series distribution to a cross machine electric field.

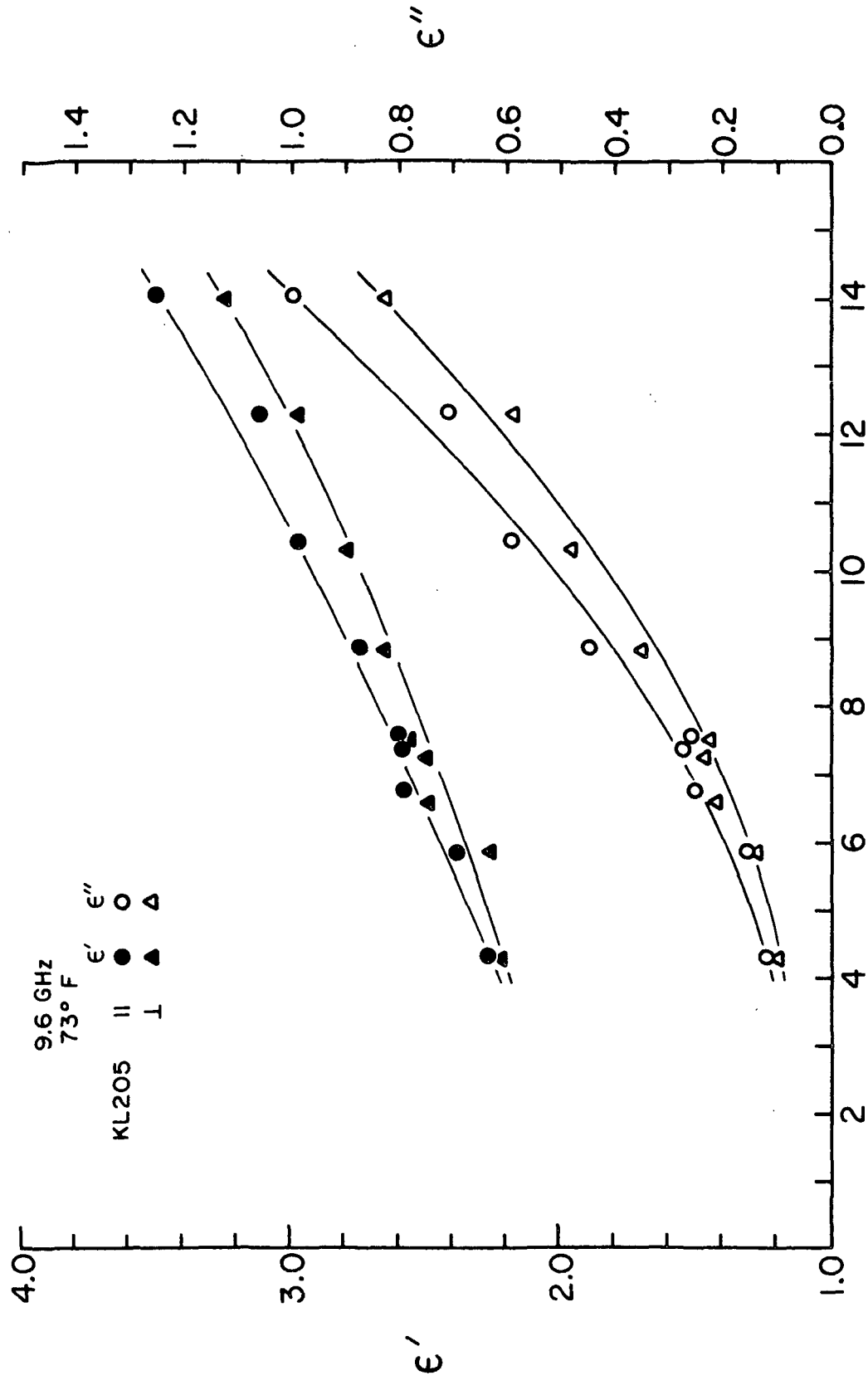

Figure 10. Dielectric Constant vs. Moisture Content and Electric Field Orientation

The pairs of curves for ε' or ε'' diverge as the moisture content increases. This is consistent with the idea that the moisture effects are dominant in paper, but that the underlying cause for the anisotropy is at the fiber level. Although the scatter in the data obscures the trend somewhat, the ratio of $\varepsilon'_{\parallel}$ to $\varepsilon'_{\perp}$ (or $\varepsilon''_{\parallel}$ to $\varepsilon''_{\perp}$) remains nearly constant over the moisture range studied.

Figure 11 illustrates the same effect by plotting permittivity versus electric field orientation for a machine made newsprint. Data such as that shown in Fig. 11 suggest that dielectric measurements offer one method for measuring the anisotropy of a machine made paper. This should be possible on moving webs, and, if the explanation offered above is correct, should be independent of moisture content. [The anisotropy ratio referred to here, of course, is not that usually defined in terms of the ratio of elastic moduli in the plane of the sheet. The latter has contributions from both fiber alignment and drying restraints. The "dielectric anisotropy," however, is believed to involve only fiber orientation effects.

Dielectric constant versus moisture curves are shown in Fig. 12 at two temperatures, 73°F and 100°F. The dielectric behavior of substances which absorb water is a complicated function of temperature. Increasing the temperature can free dipole motion and thereby raise ε'. This can also move the ε'' absorption peaks to higher frequencies and can cause increases or decreases in ε'', depending on peak locations. On the other hand, an increased temperature can lead to a greater drag on rotating dipoles and perhaps a lower ε'. In the case of liquid water at these frequencies, ε' increases and ε'' decreases with increasing temperature. Nevertheless, the observed results (both ε' and ε'' increasing) are perhaps not surprising due to the complicating influence of the absorbing medium.

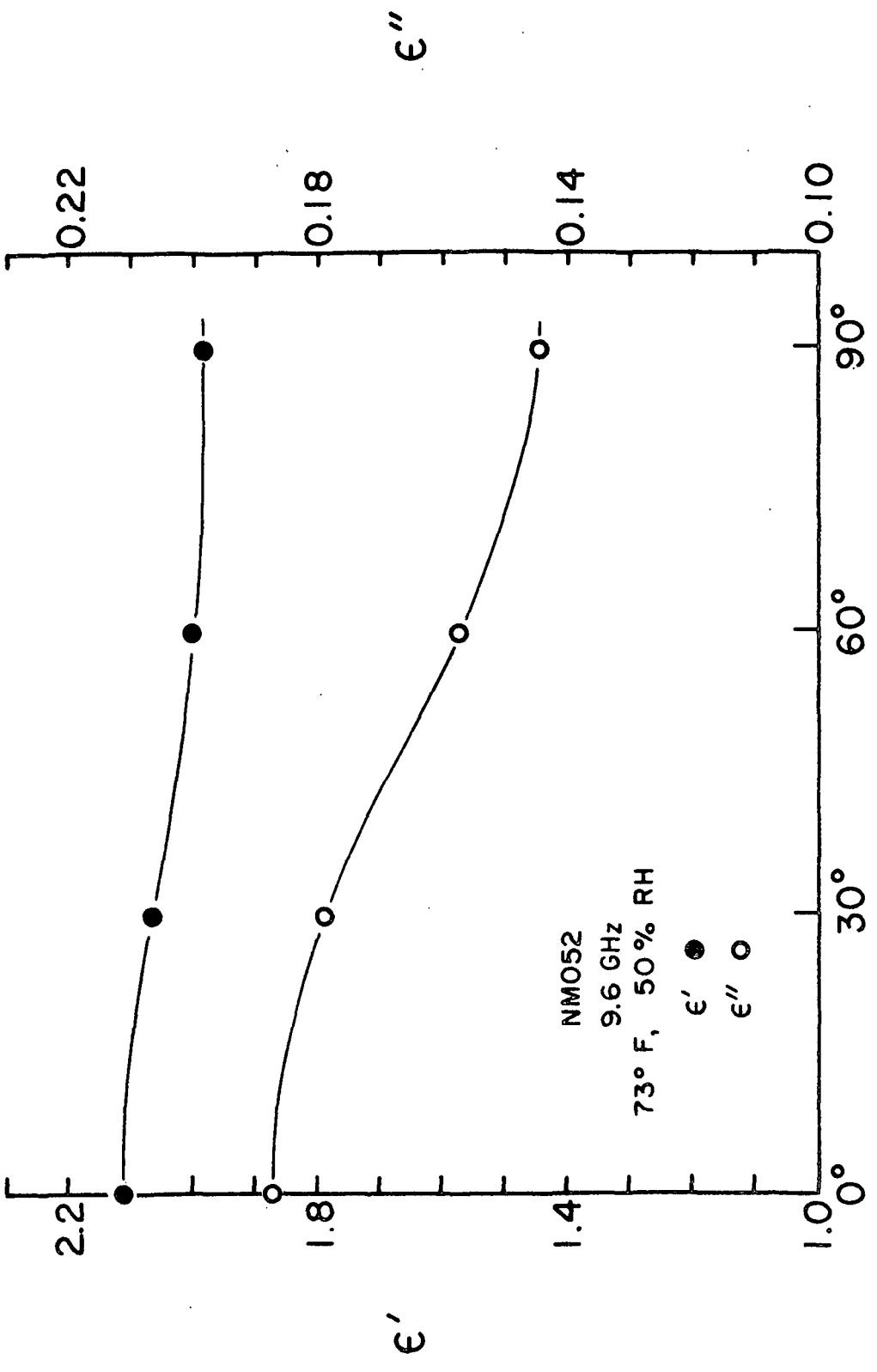

Figure 11. Dielectric Constant vs. Orientation of Electric Field

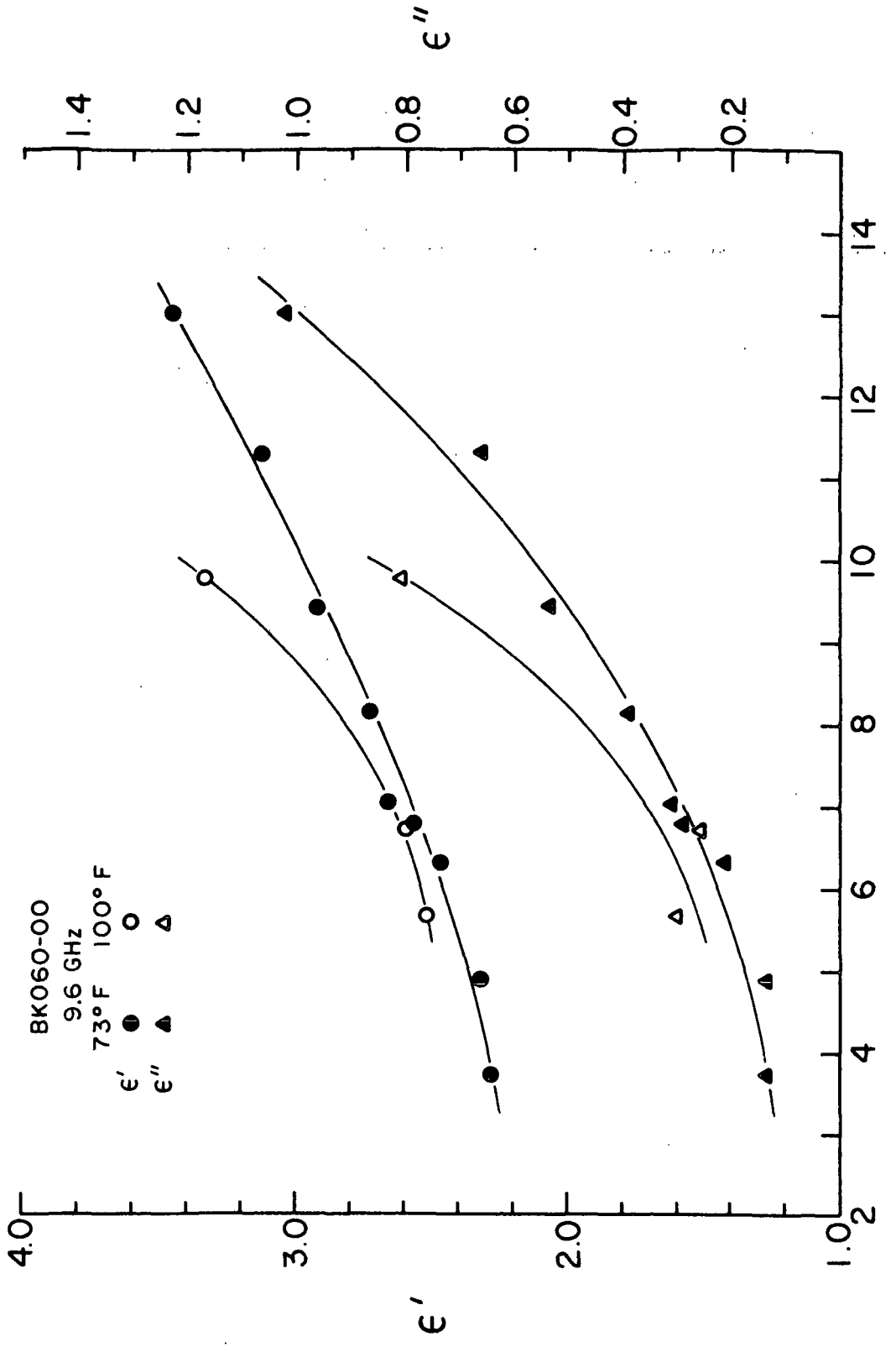

Figure 12. Dielectric Constant vs. Moisture Content and Temperature

The dielectric constant is a bulk property of a material, and thus it should not be well correlated with basis weight. Figure 13 shows dielectric constant versus moisture for four newsprint samples differing in basis weight. The effect of basis weight at low moistures is undetectable. The data at the highest moistures show a small increase of dielectric constant with basis weight.

The increase in dielectric constant due to wet pressing, refining, and calendering, is demonstrated in Fig. 14, 15, and 16, respectively. All three of these papermaking processes increase the sheet density. In general, a density increase results in a tighter packing of dipoles, and thus, a larger dielectric constant. If there is no inherent change in the dielectric properties of the wet fiber, the density change alone should account for the change in dielectric constant. In order to estimate the effect of density increase, paper is modeled as a two-phase dielectric mixture of wet fiber and air. Knowing the fiber density, the volume fraction of air, q, can be calculated from the measured values of basis weight and caliper. If the detailed geometry of the sheet were known, the effective dielectric constant of the sheet could be calculated from q, the volume fraction of air, and the dielectric constant of the fiber, ε_f. For the sake of mathematical simplicity, the sheet geometry is approximated as that of spherical air inclusions in a fiber matrix. Using this assumption, the dielectric constant of the sheet, ε, ε_f, and q can be related by the Maxwell-Garnett equation (7):

$$(2\varepsilon_f + 1)(\varepsilon_f - \varepsilon) = q(\varepsilon_f - 1)(\varepsilon + 2\varepsilon_f).$$

Using this equation, the dielectric constants of the denser sheets can be estimated from the measured dielectric constant of the least dense sheet, as follows. A value for the fiber density is assumed and the q of the low density sheet is calculated. The value of ε_f is calculated by the Maxwell-Garnett equation using q and the measured value of ε. The q of the higher density sheet is now calculated and the ε of the

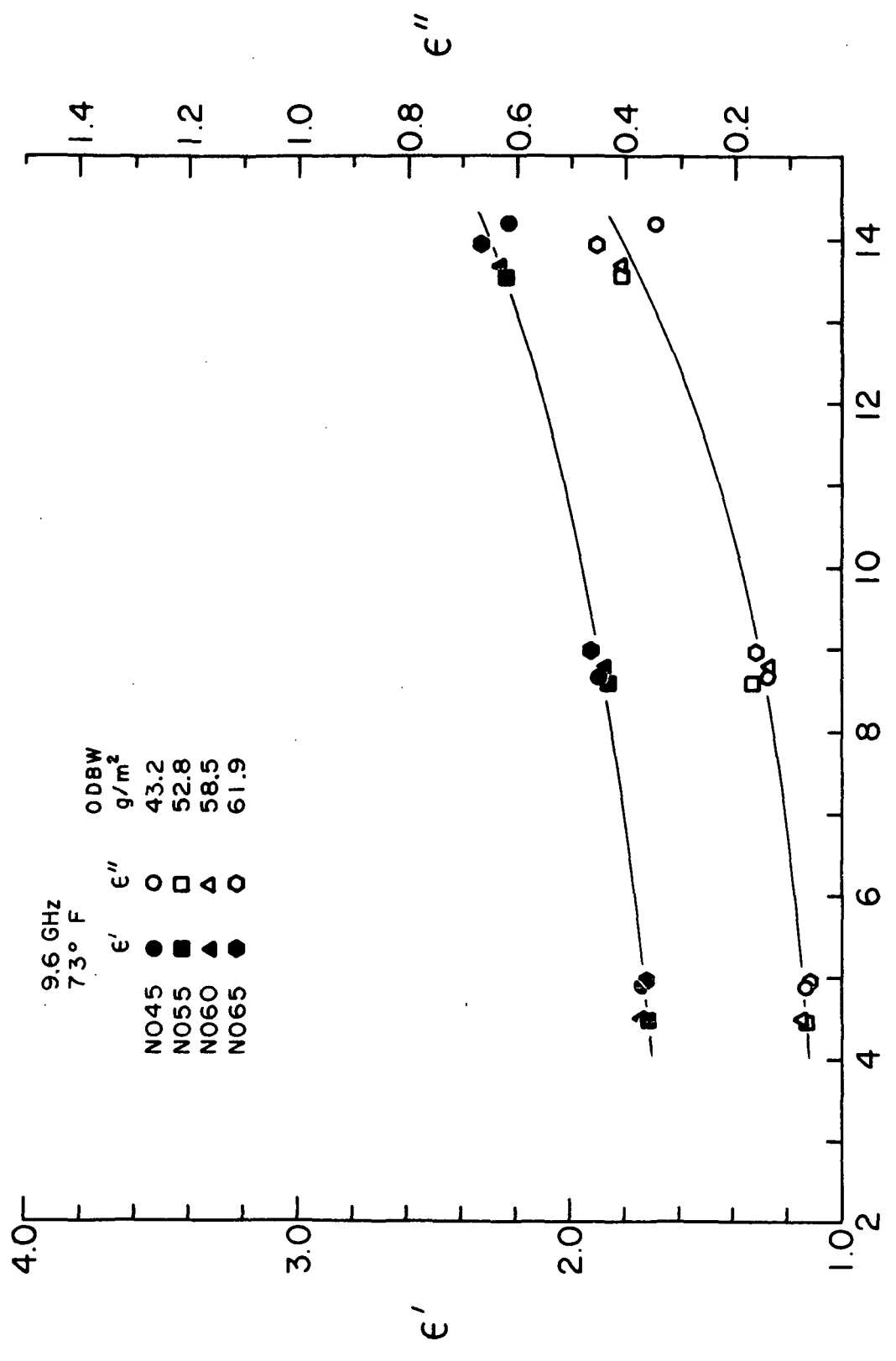

Figure 13. Dielectric Constant vs. Moisture Content and Basis Weight

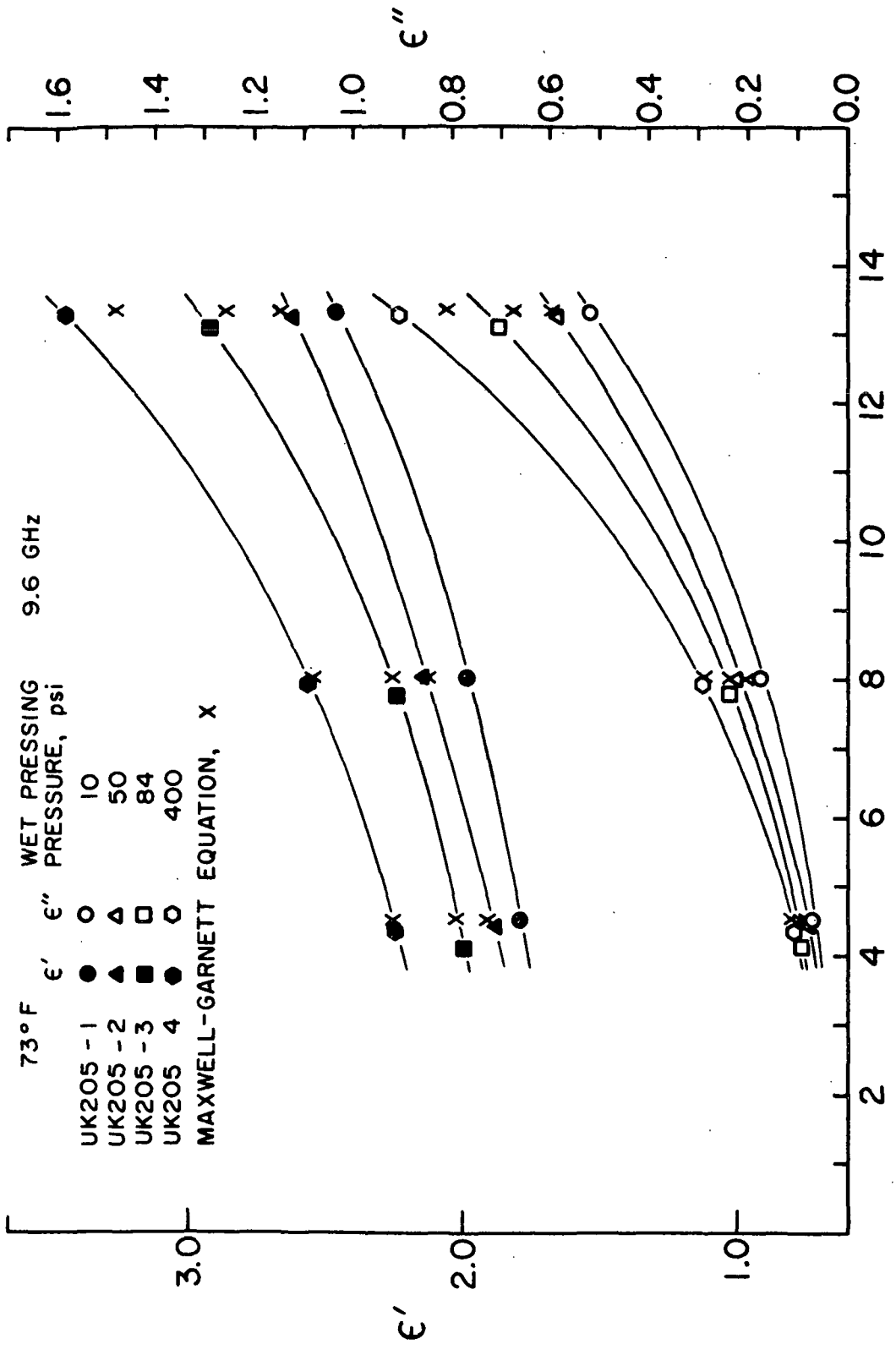

Figure 14. Dielectric Constant vs. Moisture Content and Wet Pressing

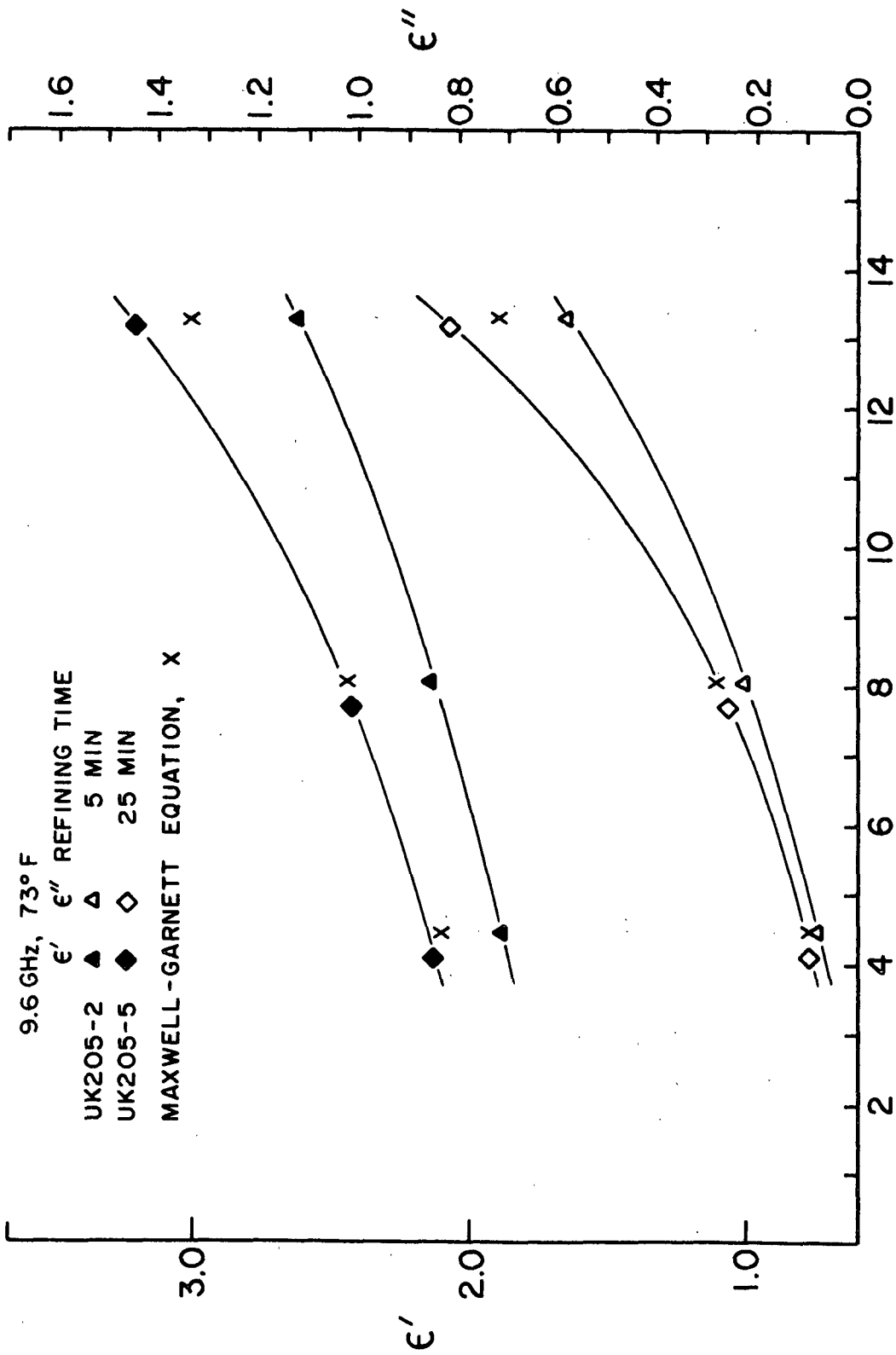

Figure 15. Dielectric Constant vs. Moisture Content and Refining

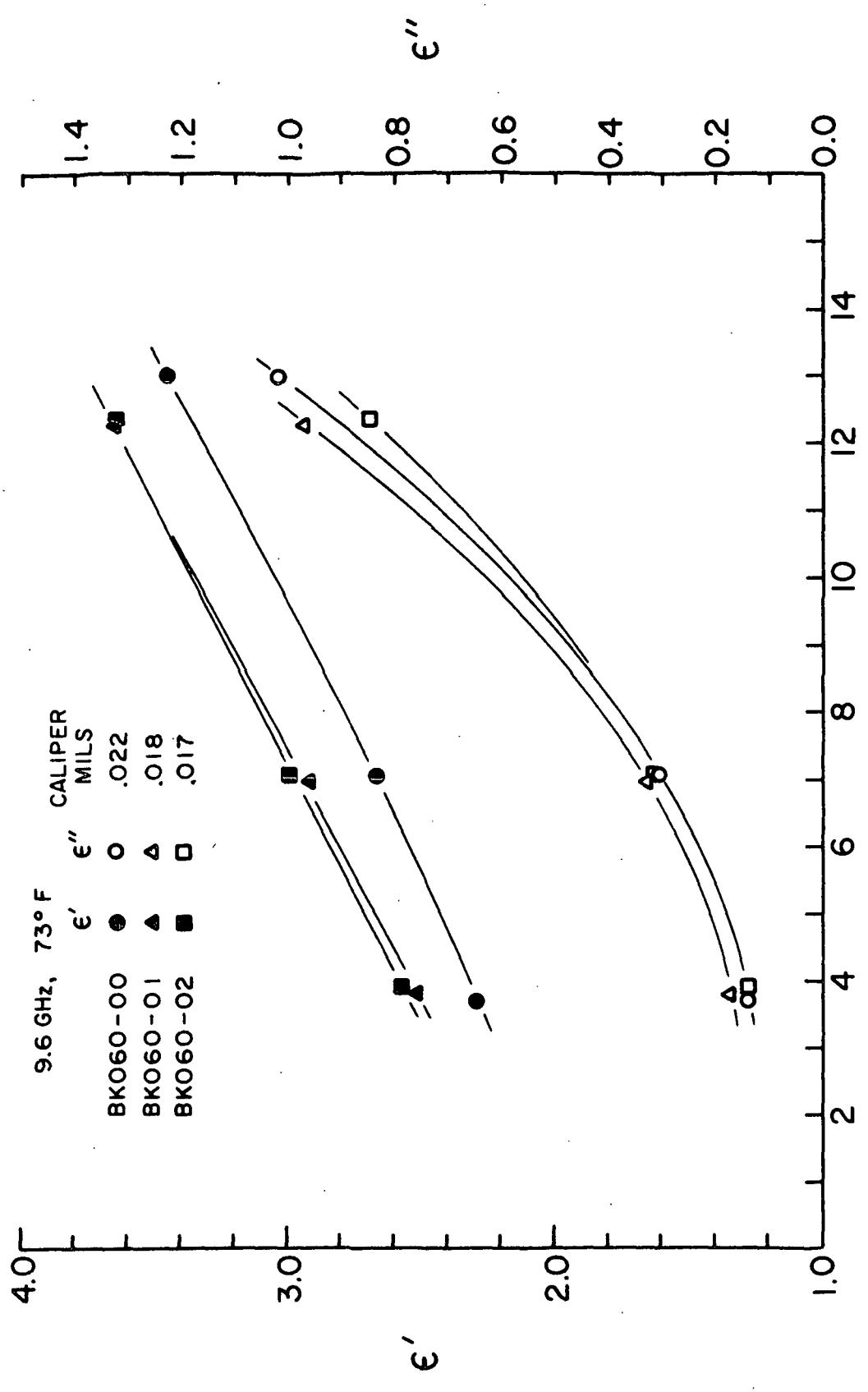

Figure 16. Dielectric Constant vs. Moisture Content and Number of Calender Passes

higher density sheet is found from the Maxwell-Garnett equation, using the ε_f calculated above. These calculations were performed for the UK205 series of samples and the results are included in Fig. 14 and 15, depicting the wet pressing and refining results, respectively. The calculated dielectric constants at each moisture agree quite favorably with the measured values, except at the highest moisture, where the calculated values fall beneath the measured. The fiber density assumed was 1.6 g/cm^3, but the calculated values were relatively insensitive to the assumed fiber density in the range 1.3 to 1.7 g/cm^3.

The generally good agreement between the predicted and measured dielectric constants is taken as evidence that the dielectric effect of wet pressing and refining is basically to change the volume fraction of air. It should be mentioned that the Maxwell-Garnett equation requires values of q small enough that connected inclusions are not occurring. This may not be the case here, where the calculated q's are in the range of 50%, assuming a fiber density of 1.6 g/cm^3. Nevertheless the agreement noted above is quite good.

The comparisons of the calculated and measured dielectric constants for the calendered samples, however, were not so good (not shown). In this case the predicted values were considerably larger than the measured ones. If these bleached kraft samples are representative of what occurs during the calendering process, the poor agreement suggests something other than a simple density change is occurring.

Figure 17 demonstrates the effect of a TiO_2 filler on the dielectric constant. Since the real part of the dielectric constant of TiO_2 (approximately 117) is larger than that of water (approximately 80), a significant increase in ε' is expected with the addition of TiO_2. The observed increase in ε', however, is small when compared to that caused by an equal weight of water. The contribution of any component to the dielectric properties of a mixture depends upon its dielectric constant, volume

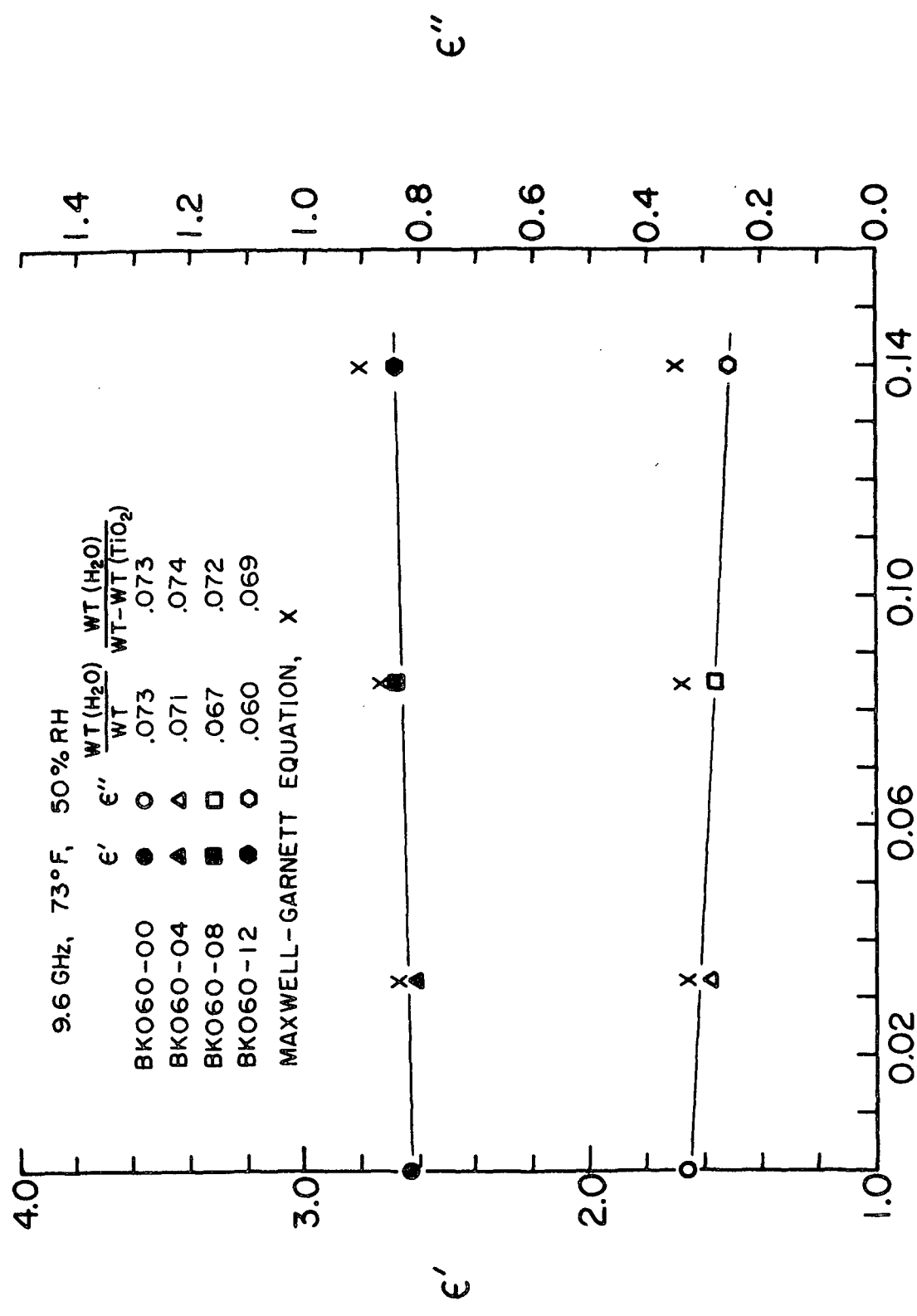

Figure 17. Dielectric Constant vs. TiO_2 Content

fraction, and geometry. The higher mass density of TiO_2 (4.26 g/cm^3) explains some of the lack of sensitivity. Perhaps more important is the fact that the TiO_2 exists as isolated clumps on the fiber, causing a smaller effect than the water which is more uniformly distributed. A more "connected" geometry leads to larger dielectric effects for much the same reasons that conductors mixed in an insulating matrix cause greater effects if they are connected.

The Maxwell-Garnett equation can also be used to estimate the effect of TiO_2 addition on the dielectric constant. This is done most easily by assuming the TiO_2 can be represented as spherical inclusions randomly distributed in a matrix having the dielectric properties of the unfilled sheet. The relationship between the dielectric constant of the filled sheet, ε, to the dielectric constant of the unfilled sheet, ε_o, and the volume fraction of TiO_2, Q, is

$$\varepsilon = \varepsilon_o(\varepsilon_T(1+2Q)+2\varepsilon_o(1-Q))/(\varepsilon_T(1-Q)+\varepsilon_o(2+Q))$$

where ε_T is the dielectric constant of TiO_2. Doping a sheet with spherical inclusions is not an effective way to change dielectric constant. It is expected, therefore, that the Maxwell-Garnett equation should underestimate the effect of the TiO_2. This is not the case, however, as the predicted increase in ε' is about three times that observed. The theory also predicts a slight increase in ε'', while the observed value actually decreases slightly. The observed behavior can be explained in terms of the change in moisture content which results from the TiO_2 addition (see Fig. 17). All the sheets were measured at the same relative humidity and the heavier doped sheets have considerably less moisture. Most of this moisture decrease is due to the decreased amount of fiber present as the TiO_2 content is increased. This is accounted for by the Maxwell-Garnett equation. Any additional moisture decrease could be due to TiO_2 obstructing water absorption sites on the fiber. In this instance, less water than

expected is found in the doped sheets resulting in lower ε'' (and ε'). In summary, it is proposed that the small effects noted when TiO_2 is added is due to the disconnected geometry of the TiO_2, and possibly the TiO_2 blocking prospective water absorption sites.

Figure 18 shows the effect of clay fillers on ε' and ε''. The graph depicts a small reduction in the dielectric constants with an increase in clay filler content. Since the measured changes are small, and the maximum clay content is only 3.5%, this trend should not be of great significance.

Figure 19 demonstrates the effect of clay coatings on the effective dielectric constant of sheets at 50% RH. The value of ε' increases noticeably, while no significant change is detected in ε''. The coating is 100 parts of a kaolin clay and 16 parts latex binder. Since this clay has a dielectric constant of only 2.6 when dry, the trend of ε' in Fig. 19 is at first puzzling. As shown on the figure, the ratio of water weight to fiber weight increases with coating weight. This indicates that the coating is holding moisture. It is presumed that this moisture causes the ε' of the coating to be greater than the ε' of the sheet, resulting in an increase in the effective ε' with coating weight.

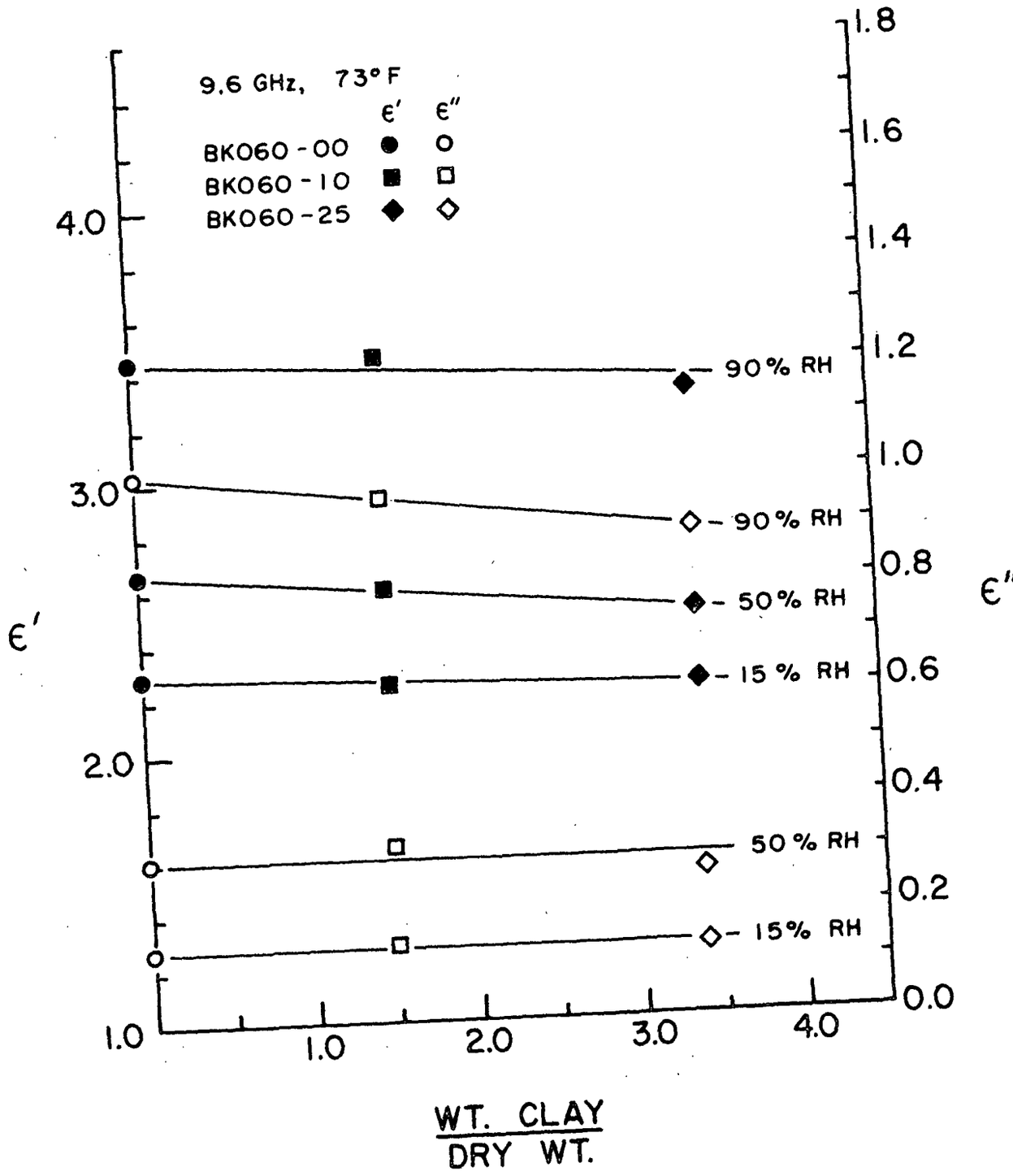

Figure 18. Dielectric Constant vs. Clay Content

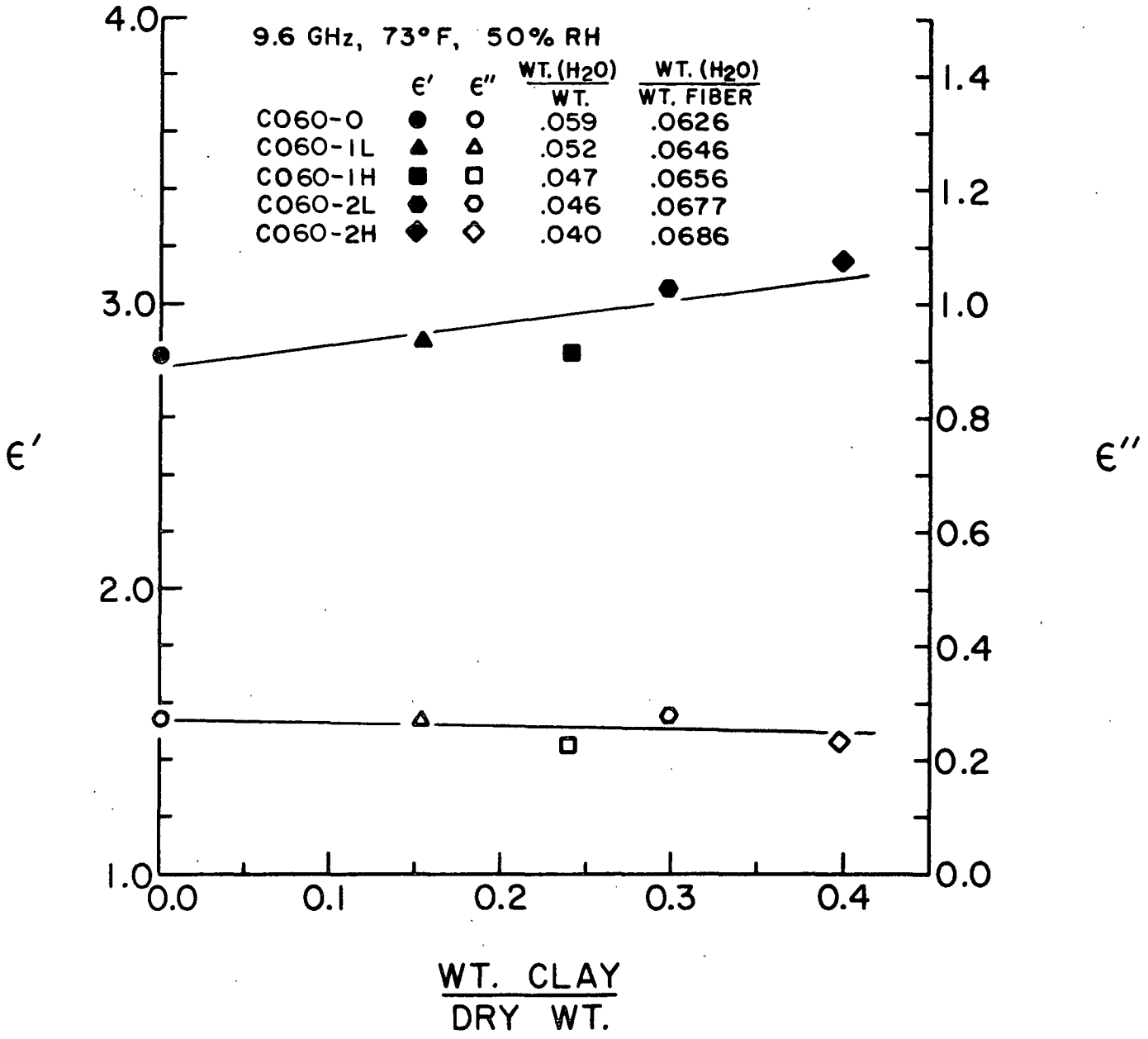

Figure 19. Dielectric Constant vs. Clay Coating

FUTURE WORK

Microwave moisture gages and microwave driers are designed to operate at high moistures. Future work on this project will extend the moisture range from about 20% moisture to near saturation. In order to make measurements at high moistures, new methods for presenting the specimens to the existing apparatus must be developed. This may require sealing conditioned specimens in thin plastic "bags" for mounting in the shorted waveguide. The effect of the bag, of course, must be accounted for. At the higher moistures, the problems of microwave drying of the specimens and moisture gradients in the specimens must be reconsidered.

ACKNOWLEDGMENTS

We are indebted to John Bachhuber for writing the computer program listed in Appendix I, and to Dave Brennan for carrying out the experimental work.

LITERATURE CITED

1. Corson, D. R. and Lorrain, P., "Introduction to Electromagnetic Fields and Waves," W. H. Freeman and Co., San Francisco and London, 1962.

2. Montgomery, C. G., Dicke, R. H., and Purcell, E. M., "Principles of Microwave Circuits," Dover Publication Inc., New York, 1965.

3. Hashin, Z. and Shtrikman, S., J. Appl. Phys. 33:3125(1962).

4. Pennock, B. E. and Schwan, H. P., J. Phys. Chem. 73(8):2600(1969).

5. Sucher, M. and Fox, J., "Handbook of Microwave Measurements," Polytechnic Press, Brooklyn, 1963.

6. Deschamps, G. A., J. Appl. Phys. 24:1004(1953).

7. Beran, M. J., "Statistical Continuum Theories," Interscience, New York, 1968.

THE INSTITUTE OF PAPER CHEMISTRY

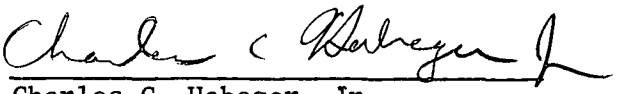

Charles C. Habeger, Jr.
Research Associate

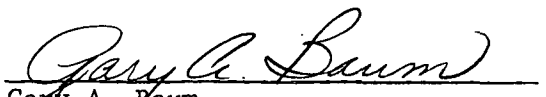

Gary A. Baum
Group Leader
Instrumentation Group

APPENDIX

The dielectric constant calculations described in the body of the report are preformed using the computer program listed below. The necessary inputs are read from statements 11 and 16. Statement 11 reads in order the following quantities: λ_{SL}(DSS); the width of the waveguide in inches (A) (.9 for all data in this report); the number of data points (N) (8 for all data in this report); sheet thickness (THK); and the micrometer reading of the probe location with no sample (BEG). The program is capable of calculating the dielectric constant using the unknown thickness or the unknown short location technique. If the value of the thickness is nonzero, the program is directed to employ the unknown short location method. If the thickness is zero, the value of the 1st short to sheet distance is assumed to be zero, and the unknown thickness calculations are made. Statement 16 reads in the values of the distance in inches between 3dB points of the standing wave minima and the micrometer setting for the minima.

The computer output includes the following in the order listed:

1. A table giving for each data point the value of the 3dB distance, the minimum location, the absolute value of the reflection coefficient, the phase of the reflection coefficient, and the X and Y component of the point;
2. The location of the center of the circle and its radius (XBAR, YBAR, and RBAR);
3. The location of 0, the intersection of the lines between opposite points (XC and YC);
4. The distance of each point from the circle;
5. The number of point nearest the circle;

6. The absolute value and phase of each component of the scattering matrix (LB_{ij} and TH_{ij});
7. The value of the calculated thickness or short location (THK or DIS);
8. The values of ε', ε'', and the loss angle along with an estimate of the maximum expected error (EP, EPP, LANG).

PROGRAM LISTING

```
  1../JOB GO
  2..C      MICROWAVE PERMITTIVITY COMPUTATIONS
  3..C      PROJ 3322  FOR CHAS. HABEGER  AUG, 1977   JJB
  4..       REAL LB(50),TH(50),DX(50),D(50),X(50),Y(50),CC(100,4)
  5..C
  6..C
  7..C      READ THE WAVELENGTH(DSS), WAVEGUIDE WIDTH(A), NO OF DATA POINTS,
  8..C       SHEET THICKNESS, AND MICROMETER ZERO SETTING
  9..C      IF THK=0, 1ST DIS. FROM SHORT  TO  SHEET  IS  SET TO ZERO AND
 10..C       EP, EPP, AND THK ARE  CALCULATED
 11..C      IF THK IS NONZERO, THK IS USED TO FIND EP, EPP, AND 1ST SHEET TO
 12..C       SHORT DISTANCE
 13..995    READ(5,9001) DSS,A,N,THK,BEG
 14..9001   FORMAT(2F10.0,I5,2F10.0)
 15..       WRITE(6,9022) DSS,A,N,THK
 16..9022   FORMAT('1DSS=',F8.6,'  A=',F8.4,'  N=',I2,'  THK=',F8.6)
 17..C      READ THE DIST BETWEEN 3DB POINTS(DX) & LOC OF MINIMUM(D)
 18..       READ(5,9002) (DX(I),D(I),I=1,N)
 19..9002   FORMAT(8F10.0)
 20..C      CALCULATE & PRINT LB & THETA(IN RADIANS)
 21..       DSSP=DSS/3.1415926
 22..       P4=4.*3.1415926/DSS
 23..       WRITE(6,9004)
 24..9004   FORMAT(' POINT',5X,'DX',13X,'D',14X,'LB',13X,'TH',13X,'X',
 25..      113X,'Y')
 26..       DO 1 I=1,N
 27..       R=SQRT(1.+1./ (SIN(DX(I)/DSSP)**2))
 28..       LB(I) = (R-1.)/(R+1.)
 29..       IF(BEG) 71,72,71
 30..71     D(I) = BEG-D(I)
 31..72     TH(I) = P4*(-D(I))
 32..       X(I) = LB(I)*COS(TH(I))
 33..       Y(I) = LB(I) * SIN(TH(I))
 34..1      WRITE(6,9003) I,DX(I),D(I),LB(I),TH(I),X(I),Y(I)
 35..9003   FORMAT(' ',I5,6(1X,F14.6))
 36..C      NOW COMPUTE THE CIRCLES FOR THE VARIOUS COMBINATIONS
 37..       CALL COMC(N,X,Y,SIGX,XB,SIGY,YB,K,RB,SIGR)
 38..C      COMPUTE CROSSING POINT OF ALL LINES
 39..       CALL CROSS(X,Y,N,CX,CY,SDX,SDY)
 40..       LOOP=1
 41..       CALL COUNT(XB,SIGX,YB,SIGY,CX,SDX,CY,SDY,CC)
 42..C      COMPUTE DIST FROM THE CIRCLE FOR EACH DATA POINT
 43..100    SMALL = RB
 44..       XB=CC(LOOP,1)
 45..       YB=CC(LOOP,2)
 46..       DO 2 I=1,N
 47..       DIST=SQRT((X(I)-XB)**2+(Y(I)-YB)**2)
 48..       DIF = RB-DIST
 49..       IF(SMALL - ABS(DIF)) 203,203,3
 50..3      SMALL = ABS(DIF)
 51..       MN=I
 52..203    IF(LOOP-1)202,202,2
 53..202    WRITE(6,9005) I,X(I),Y(I),DIST,DIF
 54..2      CONTINUE
 55..       XMP = X(MN)
 56..       YMP = Y(MN)
 57..       IF(LOOP-1) 21,21,22
 58..21     WRITE(6,9905) MN,XMP,YMP
 59..9905   FORMAT('0CLOSE POINT =',I3,'  X =',F10.6,'  Y=',F10.6)
 60..9005   FORMAT(' POINT ',I2,' X=',F8.5,' Y=',F8.5,' RADIUS =',
 61..      1 F8.5,'DIST FROM CIRCLE =',F11.4)
 62..22     OBX=CC(LOOP,3)
```

```
      OBY=CC(LOOP,4)
C     COMPUTE SLOPE AND INTERCEPT OF LINE FROM C TO OBAR
      CALL SLINT(OBX,OBY,XB,YB,BC,AC)
C     BC IS THE SLOPE, AC IS THE INTERCEPT
C     WRITE(6,9006) BC,AC
C     FORMAT(' EQ OF LINE FROM CIRCLE CENTER TO LINES INTERSECTION',
C    1/' SLOPE =',F12.8,' INTERCEPT =',F12.8)
C     COMPUTE SLOPE AND INTERCEPT OF RIGHT ANGLE LINE
      CPS   =-1./BC
      OBPS  =CPS
      CPI   = CPS  *XB*(-1)+YB
      OBPI =OBPS *OBX*(-1.)+OBY
C     WRITE(6,9007) CPS,CPI,OBPS,OBPI
C     FORMAT(' PERP TO CIRC CENTER   SLOPE =',F12.8,' INTERCEPT =',
C    1F12.8,/' LINES INTERCECTION   SLOPE =',F12.8,' INTERCEPT =',
C    2F12.8)
C     FIND THE INTERSECTION OF LINES FROM C AND OB
C     WHICH ARE PERPENDICULAR TO LINE COB, WITH THE CIRCLE
      CALL CINT(CPS,CPI,XB,RB,YB,XP,YP,XM,YM)
      XCM=XM
      YCM=YM
      CALL CINT(OBPS,OBPI,XB,RB,YB,XP,YP,XM,YM)
      XIP=XP
      YIP=YP
C     FIND THE INTERSECTION OF THESE 2 POINTS CPS=SLOPE CPI=INTERCPT
      CALL SLINT(XCM,YCM,XIP,YIP,OPS,OPI)
C     WRITE(6,9990) OPS,OPI
C     FORMAT('0SLOPE =',F12.6,' INTERCEPT =',F12.6)
C     COMPUTE X AND Y AT OPRIME
      CALL XYINT(BC,AC,OPS,OPI,XOP,YOP)
C     FIND INTERCEPT OF RT ANGLE AT XOP,YOP TO LINE COP
      OPI = CPS*XOP*(-1.) + YOP
C     FIND RLB11
      RLB11 = SQRT(XOP**2+YOP**2)
C     FIND THE ANGLE
      PI=3.1415926
      CALL ANGLE(XOP,YOP,TH11)
C      ADD PI TO ANGLE AND ADJUST
      TH11 = TH11 + PI
      IF(TH11-2.*PI) 5,5,4
4     TH11=TH11-2.*PI
C     COMPUTE DISTANCE FROM C TO OP
5     COP=SQRT((XB-XOP)**2+ (YB-YOP)**2)
      RLB22= COP/RB
C     COMPUTE INTERSECTION OF PERPINDICULAR TO OP WITH CIRCLE
      CALL CINT(CPS,OPI,XB,RB,YB,OPX,OPY,XM,YM)
C     COMPUTE DISTANCE
      OPH=SQRT((OPX-XOP)**2 + (OPY-YOP)**2)
      RLB12=OPH/SQRT(RB)
      IF(LOOP-1) 27,27,28
27    WRITE(6,9010) XOP,YOP,RLB11,TH11,RLB22,RLB12
9010  FORMAT('0O PRIME X =',F10.6,' Y =',F10.6/
     1'  LB11 =',F12.6,' TH11 =',F12.6/
     2'  LB22 =',F12.6,' LB12=',F12.6)
28    RLB22=(RLB22+RLB11)/2
C     FIND EQUATION OF LINE FROM CLOSE POINT TO O PRIME
      CALL SLINT(XMP,YMP,XOP,YOP,OSMP,OIMP)
C     FIND THE INTERSECTIONS OF THE LINE WITH THE CIRCLE
      CALL CINT(OSMP,OIMP,XB,RB,YB,XMPP,YMPP,XMPM,YMPM)
C     CHOSE THE POINT WHICH IS FARTHEST FROM XMP,YMP
      CALL FAR(XMP,YMP,XMPP,YMPP,XMPM,YMPM,XNP,YNP)
C     WRITE(6,9020) XNP,YNP
C     FORMAT('0XNP=',F12.7,'  YNP = ',F12.7)
C     FIND EQ OF LINE FROM N PRIME TO C BAR
      CALL SLINT(XNP,YNP,XB,YB,OSNP,OINP)
C     INTERSECTIONS WITH THE CIRCLE
      CALL  CINT(OSNP,OINP,XB,RB,YB,XMPL,YMPL,XMPM,YMPM)
C     CHOSE THE POINT FARTHEST FROM XNP,YNP
      CALL FAR(XNP,YNP,XMPL,YMPL,XMPM,YMPM,XMPP,YMPP)
C     WRITE(6,9021) XMPP,YMPP
C     FORMAT('0XMPP =',F12.7,'  YMPP =',F12.7)
      PHI=2.*PI*(   (MN-1.)/N)
C     FIND THE ANGLE AT WHICH MPP LIES
      CALL ANGLE(XMPP-XB,YMPP-YB,AMPP)
C     ADD PHI
      AL5=AMPP+PHI
C     ADJUST FOR 0 - 2 PI
      IF(AL5-2.*PI) 7,7,6
6     AL5=AL5-2.*PI
C     COMPUTE OBAR C LINE INTERSECTION WITH THE CIRCLE
7     CALL CINT(BC,AC,XB,RB,YB,XOCP,YOCP,XOCM,YOCM)
C     FIND POINT FARTHEST FROM O PRIME
      CALL FAR(XOP,YOP,XOCP,YOCP,XOCM,YOCM,XCPC,YOPC)
C     FIND THE ANGLE OF THIS POINT
      CALL ANGLE(XOPC-XB,YOPC-YB,AL6)
C     FIND THE DIFFERENCE BETWEEN THESE 2 ANGLES
      IF(AL6-AL5) 13,12,11
12    SG2=0.
```

```
151..       GO TO 16
152..C      L5 IS GREATER THAN L6
153..13     SG2=AL5-AL6
154..       GO TO 16
155..C      L6 IS GREATER THAN L5
156..11     SG2=2.*PI-(AL6-AL5)
157..16     SG1=AL5
158..C      WRITE(6,9031) AMPP,PHI,AL6,SG2,SG1
159..C      FORMAT('0AMPP=',F11.7,' PHI=',F11.7,' AL6=',F11.7,
160..C     1' SG2=',F11.7,' SG1=',F11.7)
161..       TH22 = SG2+PI
162..       IF(TH22-2.*PI) 15,15,14
163..14     TH22=TH22-2.*PI
164..15     TH12=SG1/2.
165..       ALNG=(TH11-TH22)*DSS/(4.*PI)
166..       DIS=ALNG/2-THK/2
167..       IF(LOOP-1) 35,35,666
168..35     IF(THK) 62,63,62
169..62     WRITE(6,9033) TH12,TH22,DIS
170..9033   FORMAT('0TH12=',F11.7,'  TH22=',F11.7,'  DIS=',F11.7)
171..       GO TO 666
172..63     WRITE(6,9030) TH12,TH22,ALNG
173..9030   FORMAT('0TH12 =',F11.7,'  TH22 =',F11.7,'  LNG =',F11.7)
174..666    CALL CPX(RLB22,RLB12,TH22,TH12,TH11,YER,YEI,THK,P4)
175..       DSS2A=(DSS/(2.*A))**2
176..       EP=(YER+DSS2A)/(1.+DSS2A)
177..       EPP=(-YEI)/(1.+DSS2A)
178..       ALSA=(ATAN(EPP/EP))*57.2956
179..       IF(LOOP-1) 700,700,702
180..700    EPM=EP
181..       EPPM=EPP
182..       ALSAM=ALSA
183..C      WRITE(6,9041) EP,EPP,ALSA,XB,YB,OBX,OBY
184..C9041  FORMAT('0FOLLOWING CORRESPOND TO CENTER CIRCLE AND LINES INTERSECT
185..C     1ION',/'0EP=',F12.7,'  EPP=',F12.7,'  LANG =',5F12.7,//)
186..       GO TO 702
187..701    WRITE(6,9040) EP,EPP,ALSA,XB,YB,OBX,OBY,LOOP
188..9040   FORMAT(' EP =',F12.7,'  EPP =',F12.7,'  L ANG=',F12.7,4F12.7,I5)
189..702    CALL RANGE(EP,EPP,ALSA,LOOP,EPB,EPS,EPPB,EPPS,ALSAB,ALSAS,
190..      1IEB,IES,IPB,IPS,IAB,IAS)
191..       LOOP=LOOP+1
192..       IF(LOOP-82)100,100,999
193..999    WRITE(6,8001) EPB,IEB,EPS,IES,EPM
194..8001   FORMAT('0LARGE AND SMALL EP =',2(F11.7,I5),'  AT CENTER EP=',F12.7
195..      1)
196..8002   FORMAT('0LARGE AND SMALL EPP=',2(F11.7,I5),'  AT CENTR EPP=',F12.7
197..      1)
198..8003   FORMAT('0LRGE AND SMALL LANG=',2(F11.7,I5),'  AT CNTR LANG=',F12.7
199..      1)
200..       WRITE(6,8002) EPPB,IPB,EPPS,IPS,EPPM
201..       WRITE(6,8003) ALSAB,IAB,ALSAS,IAS,ALSAM
202..       GO TO 995
203..       END
204..       SUBROUTINE SIMEQ(A,NR,NC)
205..C******      SOLUTION OF SIMULTANEOUS LINEAR EQUATIONS
206..C******           MATRIX OF COEFFICIENTS = A
207..C******           NR = NUMBER OF ROWS IN A
208..C******           NC = NUMBER OF COLUMNS IN A
209..       DIMENSION A(10,10),R(100)
210..       DOUBLE PRECISION A,R,D,T
211..       IF(NR - NC) 4,4,3
212..     3 NCT = NC
213..       GO TO 5
214..     4 NCT = NR
215..     5 K = 1
216..       D = 1.
217..     7 IF(A(K,K)) 12,8,12
218..C******    DIAGONAL=0, FIND A ROW WITH A NON-ZERO ELEMENT
219..C******    AND INTERCHANGE THE ROWS
220..     8 DO 9 I = K,NR
221..       IF(A(I,K)) 10,9,10
222..     9 CONTINUE
223..C******   IF THERE IS NO NON-ZERO ELEMENT, PROBLEM IS COMPLETE
224..       GO TO 17
225..C******   INTERCHANGE ROW I AND ROW K
226..    10 DO 11 J = 1,NC
227..       T = A(I,J)
228..       A(I,J) = A(K,J)
229..    11 A(K,J) = T
230..C******   CORRECT THE SYSTEM OF EQUATIONS FOR ROW K
231..    12 DO 16 I = 1,NR
232..       IF(I - K) 13,16,13
233..    13 DO 14 J = 1,NC
234..    14 R(J) = (A(I,J)*A(K,K) - A(I,K)*A(K,J))/D
235..       DO 15 J = 1,NC
236..    15 A(I,J) = R(J)
237..    16 CONTINUE
238..       D = A(K,K)
```

```
      K = K + 1
      IF(K - NCT) 7,7,17
C***     DIVIDE EACH ROW BY THE DIAGONAL ELEMENT
   17 DO 20 I = 1,NR
      DIV = A(I,I)
      IF(DIV) 18,20,18
   18 DO 19 J = 1,NC
   19 A(I,J) = A(I,J)/DIV
   20 CONTINUE
      RETURN
      END
C     COMPUTE CIRCLES FOR VARIOUS X,Y  ALL POSSIBLE, 3 AT A TIME
      SUBROUTINE COMC(N,X,Y,SIGX,XB,SIGY,YB,KT,RB,SIGR)
C     REAL X(1),Y(1),MA(10,10)
      DIMENSION MA(10,10),X(1),Y(1)
      DOUBLE PRECISION MA
C     X**X+Y**Y-2AX-2BY = R**R-A**A-B**B
C     C1=2A, C2=2B, C3=A**A+B**B-C3
      NM2=N-2
      NM1=N-1
      KT=0
      SX=0.
      SSX=0.
      SY=0.
      SSY=0.
      SR=0.
      SSR=0.
C     WRITE(6,9011)
C9001 FORMAT(' I J K',5X,'A',10X,'B',10X,'R')
      DO 1 I=1,NM2
      II=I+1
      DO 1 J=II,NM1
      IJ=J+1
      DO 1 K=IJ,N
      KT=KT+1
C     PRINT THE NODE NUMBERS AND THE X,Y COORDINATES
C     WRITE(6,9001) I,X(I),Y(I),J,X(J),Y(J),K,X(K),Y(K)
C9001 FORMAT(' ',3(I2,2X,2F14.7))
C     NOW COMPUTE THE EQUATION OF THE CIRCLE FOR THESE 3 POINTS
      MA(1,1) = X(I)
      MA(1,2) = Y(I)
      MA(1,3) = 1.
      MA(1,4) = -(X(I)**2+Y(I)**2)
      MA(2,1) = X(J)
      MA(2,2) = Y(J)
      MA(2,3) = 1.
      MA(2,4) = -(X(J)**2+Y(J)**2)
      MA(3,1) = X(K)
      MA(3,2) = Y(K)
      MA(3,3) = 1.
      MA(3,4) = -(X(K)**2+Y(K)**2)
C     SOLVE THE SIMULTANEOUS EQUATIONS
      CALL SIMEQ(MA,3,4)
C     SOLUTION IS IN COL 4
      A=MA(1,4)/2.*(-1.)
      B=MA(2,4)/2.*(-1.)
      RS=A*A+B*B-MA(3,4)
      R=SQRT(ABS(RS))
C     WRITE(6,9002) I,J,K,A,B,R
C9002 FORMAT(' ',3I2,3F11.4)
      SX=SX+A
      SY=SY+B
      SR=SR+R
      SSX=SSX+A*A
      SSY=SSY+B*B
      SSR=SSR+R*R
    1 CONTINUE
C     ALL CIRCLES HAVE BEEN COMPUTED,
C     GET AVERAGE AND STANDARD DEVIATION
      XB=SX/KT
      SIGX=SQRT(SSX/KT - XB**2)
      YB=SY/KT
      SIGY=SQRT(SSY/KT - YB**2)
      RB=SR/KT
      SIGR=SQRT(SSR/KT - RB**2)
      WRITE(6,9003) KT,XB,SIGX,YB,SIGY,RB,SIGR
 9003 FORMAT('ONUMBER OF CIRCLES COMPUTED =',I4/
     1' XBAR =',F10.6,'SIGMAX =',F10.6/
     2' YBAR =',F10.6,'SIGMAY =',F10.6/
     3' RBAR =',F10.6,'SIGMAR =',F10.6)
      RETURN
      END
      SUBROUTINE SIMEQ(A,NR,NC)
C******       SOLUTION OF SIMULTANEOUS LINEAR EQUATIONS
C******            MATRIX OF COEFFICIENTS = A
C******            NR = NUMBER OF ROWS IN A
C******            NC = NUMBER OF COLUMNS IN A
      DIMENSION A(10,10),R(100)
```

```
      SD = SD + D
      SD2 = SD2 + D**2
    2 ND = ND + 1
      AD = SD/ND
      SD = SQRT((ND*SD2 - SD**2)/ (ND*(ND-1)))
      WRITE(6,9003) ND,AD,SD
 9003 FORMAT('0NO. DIST. PTS.=',I3,', AVG. DIST.=',F8.4,
     *', SIG. D=',F8.4)
      RETURN
      END
      SUBROUTINE CINT(CCS,CCI,XB,RB,YB,
     1XCP,YCP,XCM,YCM)
C     XB AND YB = COORDINATES OF CENTER OF THE CIRCLE
C     RB = RADIUS OF THE CIRCLE
C     CCS AND CCI = SLOPE AND INTERSECT OF THE LINE
C     XC AND YCIP & M) = INTERSECTION OF LINE WITH CIRCLE
C                                   PLUS OR MINUS SQRT( B**2  - 4*A*C)
C     COMPUTE THE INTERSECTIONS OF A LINE WITH A CIRCLE
      AC=CCS**2+1.
      FKIC=CCI-YB
      BC=-2.*XB + 2.*FKIC*CCS
      CC=XB**2+FKIC**2-RB**2
      RAD=SQRT(BC**2-4.*AC*CC)
      XCP=(-BC+RAD)/(2.*AC)
      YCP=CCS*XCP+CCI
      XCM=(-BC-RAD) /(2.*AC)
      YCM=CCS*XCM+CCI
C     WRITE(6,9C01) XCP,YCP,XCM,YCM
      RETURN
C9C01 FORMAT(' SDLN FROM CENTER OF CIRCLE =',4F10.6)
      END
C     FIND THE SLOPE AND INTERCEPT OF A LINE FORMED BY 2 POINTS
      SUBROUTINE SLINT(X1,Y1,X2,Y2,OS,OI)
C     SLOPE
      OS=(Y1-Y2)/(X1-X2)
C     INTERCEPT
      OI=(Y1+Y2-OS*(X1+X2))/2.
      RETURN
      END
C     FIND THE INTERSECTION OF 2 CROSSING LINES
      SUBROUTINE XYINT(OS1,OI1,OS2,OI2,X,Y)
C     OS IS THE SLOPE, OI IS THE INTERCEPT
C     COMPUTE THE DETERMINANT
      DET=-OS1+OS2
C     X
      X=(OI1-OI2)/DET
C     Y
      Y=(OS1*(-OI2)+OS2*OI1)/DET
      RETURN
      END
      SUBROUTINE FAR(XFIX,YFIX,X1,Y1,X2,Y2,X,Y)
C     WRITE(6,9C01) XFIX,YFIX,X1,Y1,X2,Y2
C9001 FORMAT('0FIX =',2F10.6,' FIRST POINT =',2F10.6,
C    1' SECOND POINT =',2F10.6)
C     FIND THE POINT WHICH IS FARTHEST FROM XFIX,YFIX
C     AND RETURN IT IN X,Y
      D1=SQRT((XFIX-X1)**2 + (YFIX-Y1)**2 )
      D2=SQRT((XFIX-X2)**2 + (YFIX-Y2)**2 )
      IF(D1-D2) 1,1,2
    1 X=X2
      Y=Y2
      GO TO 3
    2 X=X1
      Y=Y1
    3 RETURN
      END
C     PERFORM THE NECESSARY COMPLEX ARITHMETIC
      SUBROUTINE CPX(RLB22,RLB12,TH22,TH12,TH11,YER,YEI,THK,P4)
      IF(THK) 4,5,4
    4 SP11PR=RLB22*COS((TH11+TH22)/2-P4*THK/2)
      SP11PI=RLB22*SIN((TH11+TH22)/2-P4*THK/2)
      TH=TH12-THK*P4/2
      I=0
      GO TO 6
    5 SP11PR=RLB22*COS(TH22)
      SP11PI=RLB22*SIN(TH22)
C     WRITE(6,9003) SP11PR,SP11PI
C     FORMAT('0SP11 =',2F12.7)
C     SET COUNTER TO 0
      I=0
      TH=TH12+(TH22-TH11)/2.
    6 SP12R=RLB12*COS(TH)
      SP12I=RLB12*SIN(TH)
C     WRITE(6,9C04) TH,SP12R,SP12I
C     FORMAT('0TH =',F12.7,'  SP12 =',2F12.7)
C     FORM YE
C     SQUARE 1. - SP11P
   10 CALL CMUL(1.-SP11PR,-SP11PI,1.-SP11PR,-SP11PI,SPPR,SPPI)
```

```
503..C      WRITE(6,9005) SPPR,SPPI
504..C      FORMAT('0(1-SP11P)**2 =',2F12.7)
505..C      SQUARE SP12
506..       CALL CMUL(SP12R,SP12I,SP12R,SP12I,SPRR,SPRI)
507..C      WRITE(6,9006) SPRR,SPRI
508..C      FORMAT('0SP12**2 =',2F12.7)
509..C      FORM THE NUMERATOR
510..       YEPNR=SPPR-SPRR
511..       YEPNI = SPPI-SPRI
512..C      FORM THE DENONINATOR
513..       CALL CMUL(1.+SP11PR,SP11PI,1.+SP11PR,SP11PI,SPPR,SPPI)
514..C      WRITE(6,9007) SPPR,SPPI
515..C      FORMAT('0(1+SP11P)**2 =',2F12.7)
516..       YEPDR=SPPR-SPRR
517..       YEPDI=SPPI-SPRI
518..C      WRITE(6,9008) YEPNR,YEPNI
519..C9008  FORMAT('0YEP NUMERATOR =',2F12.7)
520..C      WRITE(6,9009) YEPDR,YEPDI
521..C      FORMAT('0YEP DENOMINATOR =',2F12.7)
522..C      FORM THE QUOTIENT
523..       CALL CDIV(YEPNR,YEPNI,YEPDR,YEPDI,YER,YEI)
524..C      WRITE(6,9001) YER,YEI
525..C9001  FORMAT('0YE REAL =',F11.7,'  YE IMAG =',F11.7)
526..C      IF REAL PART OF YE IS GT  ONE , WE ARE DONE,  RETURN
527..       IF(YER-1.)2,1,1
528..1      RETURN
529..C      HAVE WE COME HERE BEFORE
530..2      IF(I) 20,20,99
531..C      CHANGE SIGN ON SP11P AND DO IT AGAIN
532..20     I=1
533..       IF(THK) 51,50,51
534..51     SP11PR=-RLB22*COS((TH11-TH22)/2-P4*THK/2)
535..       SP11PI=-RLB22*SIN((TH11-TH22)/2-P4*THK/2)
536..       GO TO 10
537..50     SP11PR=-SP11PR
538..       SP11PI=-SP11PI
539..       GO TO 10
540..C      NO POSITIVE REAL PART, Q U I T
541..99     WRITE(6,9002) YER,YEI
542..9002   FORMAT('0NO POSITIVE REAL PART',
543..      1/' YE REAL =',F11.7,'  YE IMAG =',F11.7)
544..       CALL EXIT
545..       END
546..C      MULTIPLY 2 COMPLEX NUMBERS
547..C      X*Y = RX*RY - IX*IY + IX*RY + IY*RX
548..C      REAL PART = FIRST HALF, IMAGINARY = SECOND HALF
549..       SUBROUTINE CMUL(RX,IX,RY,IY,RR,IR)
550..       REAL IX,IY,IR
551..       RR=RX*RY - IX*IY
552..       IR=IX*RY + IY*RX
553..       RETURN
554..       END
555..C      DIVIDE 2 COMPLEX NUMBERS
556..C      X/Y = RX*RY+IX*IY/(RY**2+IY**2)       REAL PART
557..C            IX*RY-RX*IY/(RY**2+IY**2)       IMAG PART
558..       SUBROUTINE CDIV(RX,IX,RY,IY,RR,IR)
559..       REAL IX,IY,IR
560..       DIV=RY**2+IY**2
561..       RR=(RX*RY+IX*IY)/DIV
562..       IR=(IX*RY-RX*IY)/DIV
563..       RETURN
564..       END
565..       SUBROUTINE COUNT(XB,SIGX,YB,SIGY,CX,SDX,CY,SDY,CC)
566..       DIMENSION CC(100,4)
567..C      COMPUTE AND STORE IN CC VARIABLE + OR - STD DEV
568..       CC(1,1) = XB
569..       CC(1,2) = YB
570..       CC(1,3) = CX
571..       CC(1,4) = CY
572..       XC=XB-2.*SIGX
573..       LOOP=2
574..       DO 1 I=1,3
575..       XC=XC+SIGX
576..       YC=YB-2.*SIGY
577..       DO 1 J=1,3
578..       YC=YC+SIGY
579..       XI=CX-2.*SDX
580..       DO 1 K=1,3
581..       XI=XI+SDX
582..       YI=CY-2.*SDY
583..       DO 1 L=1,3
584..       YI=YI+SDY
585..       CC(LOOP,1) = XC
586..       CC(LOOP,2) = YC
587..       CC(LOOP,3) = XI
588..       CC(LOOP,4) = YI
589..1      LOOP=LOOP+1
590..       RETURN
```

```
591..        END
592..C       COMPUTE THE ANGLE OF THE POINT X,Y
593..        SUBROUTINE ANGLE(X,Y,A)
594..        PI=3.1415926
595..C       CHECK X
596..        IF(X) 10,20,2
597..C       X IS POSITIVE
598..2       A=ATAN(Y/X)
599..        IF(Y) 5,6,6
600..C       Y IS NEGATIVE, ADD 2 PI
601..5       A=A+2.*PI
602..6       RETURN
603..C       X IS ZERO, CHECK Y
604..20      IF(Y) 21,23,22
605..C       Y NEG, ANGLE IS 3 PI OVER 2
606..21      A = 3.*PI/2.
607..        RETURN
608..22      A=PI/2.
609..        RETURN
610..C X AND Y ARE ZERO, ANGLE UNDEFINED
611..23      WRITE(6,9001)
612..9001    FORMAT('0X AND Y ARE ZERO, ANGLE UNDEFINED')
613..        A=0.
614..        RETURN
615..C       X IS NEGATIVE, ADD PI
616..10      A=ATAN(Y/X)+PI
617..        RETURN
618..        END
619..C       FIND THE LARGEST AND SMALLEST, AND FIND THE LOOP WHERE IT HAPPENED
620..        SUBROUTINE RANGE(EP,EPP,AL,LOOP,EPB,EPL,EPPB,EPPL,ALB,ALL,
621..       1IEB,IEL,IPB,IPL,IAB,IAL)
622..        IF(LOOP-1) 1,1,10
623..1       EPB=EP
624..        IEB=LOOP
625..        EPL=EP
626..        IEL=LOOP
627..        EPPB=EPP
628..        IPB=LOOP
629..        EPPL=EPP
630..        IPL=LOOP
631..        ALB=AL
632..        IAB=LOOP
633..        ALL=AL
634..        IAL=LOOP
635..        RETURN
636..C       FIND BIG AND SMALL
637..10      CALL RAN(EP,EPB,EPL,IEB,IEL,LOOP)
638..        CALL RAN(EPP,EPPB,EPPL,IPB,IPL,LOOP)
639..        CALL RAN(AL,ALB,ALL,IAB,IAL,LOOP)
640..        RETURN
641..        END
642..        SUBROUTINE RAN(A,AB,AL,IB,IL,LOOP)
643..        IF(A-AB) 1,10,6
644..C       AB IS LARGER, CHECK FOR SMALLEST
645..1       IF(A-AL) 2,10,10
646..C       WE HAVE A SMALLER ITEM
647..2       AL=A
648..        IL=LOOP
649..        RETURN
650..C       AB IS SMALLER
651..6       AB=A
652..        IB=LOOP
653..10      RETURN
654..        END
```

COMPUTER OUTPUT SAMPLE

DSS=1.686000 A= 0.9000 N= 8 THK=0.019800

POINT	DX	D	LB	TH	X	Y
1	0.003200	0.003100	0.988146	-0.023106	0.987882	-0.022830
2	0.013500	0.127900	0.950944	-0.953285	0.550604	-0.775326
3	0.026400	0.259500	0.906372	-1.934148	-0.322133	-0.847196
4	0.030700	0.378900	0.892004	-2.824079	-0.847417	-0.278489
5	0.026300	0.479200	0.906709	-3.571651	-0.824145	0.378029
6	0.017300	0.566700	0.937584	-4.223821	-0.440066	0.827892
7	0.008700	0.650600	0.968101	-4.849158	0.131994	0.959060
8	0.002500	0.740900	0.990727	-5.522197	0.717439	0.683242

NUMBER OF CIRCLES COMPUTED = 56
XBAR = 0.046854SIGMAX = 0.001232
YBAR = 0.020555SIGMAY = 0.001174
RBAR = 0.942409SIGMAR = 0.002380

1	0.9879	-0.0228	-0.8241	0.3780	-0.2212	0.1957		
2	0.5506	-0.7753	-0.4401	0.8279	-1.6183	0.1157	-0.0573	0.2084
1	0.9879	-0.0228	-0.8241	0.3780	-0.2212	0.1957		
3	-0.3221	-0.8472	0.1320	0.9591	3.9774	0.4341	-0.0568	0.2083
1	0.9879	-0.0228	-0.8241	0.3780	-0.2212	0.1957		
4	-0.8474	-0.2785	0.7174	0.6832	0.6146	0.2423	-0.0558	0.2080
2	0.5506	-0.7753	-0.4401	0.8279	-1.6183	0.1157		
3	-0.3221	-0.8472	0.1320	0.9591	3.9774	0.4341	-0.0569	0.2078
2	0.5506	-0.7753	-0.4401	0.8279	-1.6183	0.1157		
4	-0.8474	-0.2785	0.7174	0.6832	0.6146	0.2423	-0.0567	0.2075
3	-0.3221	-0.8472	0.1320	0.9591	3.9774	0.4341		
4	-0.8474	-0.2785	0.7174	0.6832	0.6146	0.2423	-0.0570	0.2073

COORDINATES OF THE INTERSECTION

XC = -0.0567, YC = 0.2079, SDX=0.000514, SDY=0.000504

NO. DIST. PTS.= 15, AVG. DIST.= 0.0009, SIG. D= 0.0004

POINT 1	X= 0.98788	Y=-0.02283	RADIUS = 0.94203	DIST FROM CIRCLE =	0.0004
POINT 2	X= 0.55060	Y=-0.77533	RADIUS = 0.94191	DIST FROM CIRCLE =	0.0005
POINT 3	X=-0.32213	Y=-0.84720	RADIUS = 0.94294	DIST FROM CIRCLE =	-0.0005
POINT 4	X=-0.84742	Y=-0.27849	RADIUS = 0.94295	DIST FROM CIRCLE =	-0.0005
POINT 5	X=-0.82415	Y= 0.37803	RADIUS = 0.94150	DIST FROM CIRCLE =	0.0009
POINT 6	X=-0.44007	Y= 0.82789	RADIUS = 0.94281	DIST FROM CIRCLE =	-0.0004
POINT 7	X= 0.13199	Y= 0.95906	RADIUS = 0.94236	DIST FROM CIRCLE =	0.0001
POINT 8	X= 0.71744	Y= 0.68324	RADIUS = 0.94278	DIST FROM CIRCLE =	-0.0004

CLOSE POINT = 7 X = 0.131994 Y= 0.959060

O PRIME X = -0.005624 Y = 0.115453
LB11 = 0.115590 TH11 = 4.761066
LB22 = 0.115069 LB12= 0.964329

TH12= 3.0251226 TH22= 3.9743109 DIS= 0.0428785

LARGE AND SMALL EP =	2.6586304	49	2.6056108	17	AT CENTER EP=	2.6263790
LARGE AND SMALL EPP=	0.3389308	82	0.2798579	2	AT CENTR EPP=	0.3090332
LRGE AND SMALL LANG=	7.3276520	80	6.0894690	4	AT CNTR LANG=	6.7108297